The Thesis Committee for Yubing Wang
Certifies that this is the approved version of the following thesis:

Influence of Ground Motion Scaling Methods on the Computed Seismically-Induced Sliding Displacements of Slopes

APPROVED BY
SUPERVISING COMMITTEE:

Super

Ellen M. Rathje

Chadi El Mohtar

Influence of Ground Motion Scaling Methods on the Computed Seismically-Induced Sliding Displacements of Slopes

by

Yubing Wang, B.E.

Thesis

Presented to the Faculty of the Graduate School of

The University of Texas at Austin

in Partial Fulfillment

of the Requirements

for the Degree of

Master of Science in Engineering

The University of Texas at Austin

December 2010

Acknowledgements

I would like to thank Dr. Ellen M. Rathje for her efforts and encouragement during the preparation of this thesis. I appreciate the opportunity of working with my supervisor, Dr. Rathje. Her significant contribution of time and knowledge to this thesis is gratefully acknowledged. I also want to thank Dr. Chadi El Mohtar for his time and valuable comments on this thesis.

I am grateful for Dr. Albert Kottke, who offered many helps on the ground motions used in this study. I am thankful for Dr. Randall W. Jibson, who provided a program for computing the sliding displacements.

I want to thank my parents for their unconditional encouragement, financial support and love. I also thank for my friend Wupeng Yan, who gave me many great suggestions.

I also want to thank my friends for brightening my life.

December 3, 2010

Abstract

Influence of Ground Motion Scaling Methods on the Computed Seismically-Induced Sliding Displacements of Slopes

Yubing Wang, MSE

The University of Texas at Austin, 2010

Supervisor: Ellen M. Rathje

Evaluation of the seismic stability of slopes often involves an estimate of the expected sliding displacements. This evaluation requires a suite of acceleration-time histories as input motions. The methods of selecting and scaling these motions can affect the computed sliding displacements. Linear scaling of recorded ground motions and modification of recorded motions by spectral matching are common approaches used for ground motion selection and these approaches were used in this study to select motions for use in sliding displacement analyses. Rigid sliding block analyses and decoupled flexible sliding block analyses were performed using a suite of linearly scaled motions and a suite of spectrally matched motions. . Generally, the spectrally matched motions predict 10 to 30%, on average, smaller displacements and significantly less variability than the linearly scaled motions, when both suites of input motions were developed to match the same acceleration response spectrum. When both

suites of input motions were developed to match the same peak ground velocity and acceleration response spectrum, the spectrally matched motions generally predict 5 to 15%, on average, larger displacements than the linearly scaled motions. Because ground motion parameters beyond acceleration response spectrum affect the computed sliding displacement, parameters such as peak ground acceleration (PGA), peak ground velocity (PGV) and mean period (T_m) should be considered in selecting and scaling motions for use in sliding displacement analyses.

Table of Content

List of Tables

List of Figures

Chapter 1 Introduction

1.1 RESEARCH SIGNIFICANCE

Stability can be an issue in both natural slopes and man-made slopes. Most slopes are stable under static conditions, but when an earthquake occurs the seismically-induced ground shaking is often sufficient to cause failures of slopes which were marginally to moderately stable under static conditions.

Tremendous amounts of damage have been caused by earthquake-induced landslides in previous earthquake. In some earthquakes, landslides have been responsible for equal to or even more than half of the total damage caused by all the seismic hazards. In the 1964 Alaska earthquake, earthquake-induced landslides caused an estimated 56% of the total cost of damage (Youd, 1978; Wilson and Keefer, 1985). More than half of all deaths in large (M>6.9) earthquakes in Japan between 1964 and 1980 were caused by landslides (Kobayashi, 1981). The 1920 Haiyuan earthquake (M=8.5) in the Ningxia Province of China induced hundreds of large landslides, which took away 100,000 lives (Close and McCormick, 1922). More recently, the 2008 Sichuan Earthquake in China induced significant landslides and these landslides not only buried dozens of towns, but also blocked roads, which are the lifelines connecting those ruined towns and nearby large cities. Thus, the evaluation of the seismic stability

of slopes is an important activity for geotechnical engineers.

Evaluation of the seismic stability of slopes often involves an estimate of the expected sliding displacement induced by earthquake shaking. This evaluation requires a suite of acceleration-time histories to use as input into the sliding displacement analysis. However, the selected motions and the manner in which they are scaled may significantly affect the computed sliding displacement.

In this study, two main approaches to ground motions selection are considered. These approaches are the linear scaling process and the spectral matching process. The linear scaling approach involves simply multiplying an acceleration-time history by a scale factor that linearly scales the intensity of the motion and its acceleration response spectrum. The frequency content of the motion is not modified. The spectral matching approach involved modifying the acceleration-time in the time domain such that the time series meet specific response spectra characteristics. The influence of these approaches on the computed seismically-induced sliding displacements of slopes is investigated.

1.2 SCOPE

After this introduction in Chapter 1, the methods for evaluating earthquake-induced sliding displacement are introduced in Chapter 2. The original Newmark (1965) rigid-block analysis is discussed, along with the assumptions and

limitations of this method. Another modified Newmark-type sliding block method (i.e. decoupled analysis), which accounts for the flexibility of the sliding mass, is also introduced. The two main approaches to ground motion scaling, which are linear scaling and spectral matching, to modifying recorded ground motions are explained.

Chapter 3 describes the site analyzed in this study and the suites of ground motion used as input into the dynamic response and sliding analyses. The numerical model used for the dynamic response and sliding analyses is also described.

In Chapter 4, sliding displacements are computed for rigid and flexible sliding masses. A series of comparisons are provided, including comparisons of sliding displacements computed from different scaling methods and comparisons using different values of yield critical acceleration k_y.

Chapter 5 presents the summary and conclusions.

Chapter 2 Sliding Displacement Analyses

2.1 INTRODUCTION

The methods for evaluating the stability of slopes during earthquakes have evolved gradually since the middle of the twentieth century, when the first efforts for estimating the influence of seismic shaking on slopes were initiated.

Terzhagi (1950) developed a static limit-equilibrium analysis based on adding an earthquake force to the sliding mass. His concept was so valuable that it was widely known and accepted as pseudo-static analysis (Jibson, 2010). A few years later, the finite element method (FEM), which is also known as stress-deformation analysis, was developed and applied to slope stability analysis. However, FEM was extremely complex and needed significant computational power which was not readily available. To bridge the gap between these two types of analysis, a method called rigid sliding block analysis was recommended by Newmark (1965) for assessing the displacement of slopes during earthquakes. This method improved some of the simple assumptions of pseudo-static analysis but remained relatively simple to apply in practice. Later, Newmark's analysis was enhanced to allow for more complicated and realistic field models, which led to decoupled and fully coupled displacement analyses. In this study, rigid block and decoupled sliding analyses are applied to different site conditions.

2.2 RIGID- SLIDING BLOCK ANALYSIS

Rigid sliding block analysis to assess the seismic stability of slopes was originated from Newmark (1965). Figure 2.1 shows a schematic of Newmark's calculation procedure, and Figure 2.2 shows the conceptual model of a rigid sliding block. Sliding starts when the acceleration-time history exceeds the yield critical acceleration (k_y), which is defined as the acceleration that when multiplied by the weight of the sliding mass results in a factor of safety of 1.0. Sliding continues until the relative velocity between the sliding block and base drops back to zero. To calculate the relative displacement between the sliding block and base, the relative acceleration-time history is integrated twice with respect to time in the ranges where sliding occurs (Figure 2.1). At point X, where the ground acceleration reaches the level of yield critical acceleration, the sliding starts. The relative acceleration between the base and k_y is integrated to obtain the relative velocity, and the relative velocity is integrated to obtain the relative sliding displacement. At point Y, the ground acceleration decreases to the k_y level, but the sliding does not stop due to non-zero relative velocity. At point Z, the relative velocity becomes zero and the sliding stops. Sliding is triggered again when the ground acceleration exceeds the k_y level.

A key assumption of Newmark's method is that the sliding mass is treated as a

rigid block, which means no internal deformation occurs within the sliding mass. Thus, there is no flexibility or dynamic response of the material above the sliding surface. For slopes with shallow failure surfaces, which are very common in natural slopes subjected to earthquake motion (Keefer, 1984), the differences of deformation within the sliding mass are so small that they can be neglected and the rigid block assumption is valid. However, deep slope failures are common in man-made earth structures, and the internal deformations of these slopes cannot be ignored.

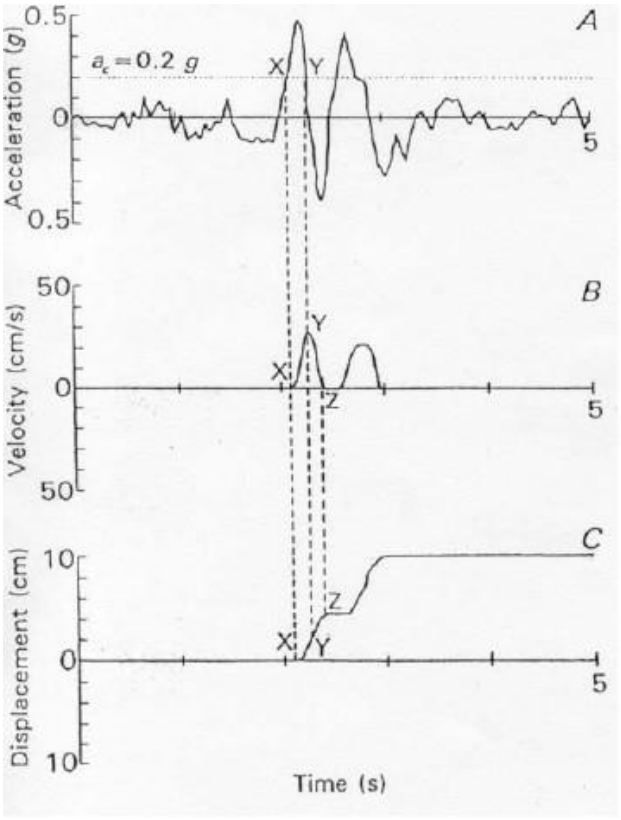

Figure 2.1 Calculation of Permanent Sliding Displacement with Newmark Rigid Block Sliding Procedure (Jibson, 1993) (Note that Jibson represented yield critical acceleration k_y as a_c)

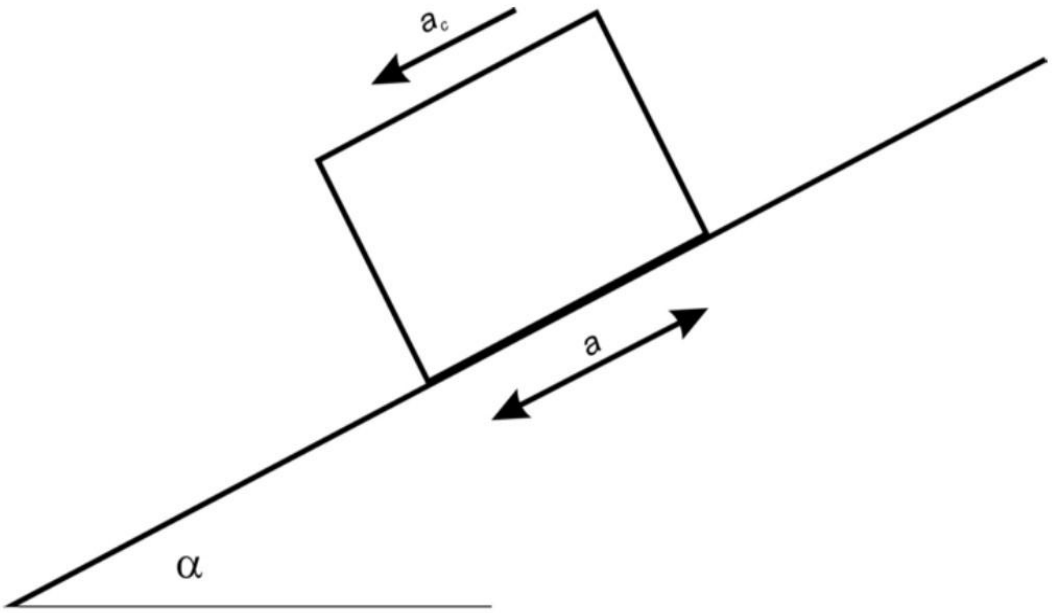

Figure 2.2 Newmark's Rigid-block Model for Slopes (Jibson, 1993) (Note that Jibson represented yield critical acceleration k_y as a_c)

2.3 DECOUPLED ANALYSIS AND DYNAMIC RESPONSE

For deeper failure surfaces in earth structures, the internal deformation and the flexibility of the sliding mass cannot be neglected during seismic shaking (Seed and Martin 1966, Lin and Whitman 1983). Decoupled analysis was developed to account for the deformability of sliding masses (Makdisi and Seed 1978). This decoupled analysis can be divided into two steps. (1) A dynamic response analysis and (2) a sliding displacement analysis. In the dynamic response analysis, a series of acceleration-time histories at several points within the earth structure are computed and an average acceleration-time history (called a k-time history) for the sliding mass is calculated. Alternatively, the k-time history can be derived from the

seismically-induced stresses along the sliding surface (Chopra 1967). The k-time history represents the seismic force for the sliding mass and thus is an appropriate measure of the seismic loading. The maximum value of k-time history is called k_{max}. In the sliding displacement analysis, the k-time history is used in a rigid sliding block analysis in lieu of the original acceleration-time history. This decoupled sliding block approach (e.g., Makdisi and Seed 1978, Bray and Rathje 1998) computes the dynamic response of the sliding mass without any consideration of the sliding displacement, and then uses the results of the dynamic response analysis to compute the sliding displacement. Because the dynamic response analysis and computation of the sliding displacement are performed independently, this method is called a decoupled analysis. Figure 2.3 schematically compares rigid and decoupled sliding block analyses, and Figure 2.4 demonstrated the differences in the computed seismic loading time histories for rigid and decoupled sliding block analyses. For rigid sliding the acceleration-time history beneath the block is used as the seismic loading in the sliding displacement analysis, while for decoupled analysis of a flexible sliding mass the k-time history is used as the seismic loading. Note that the schematic in Figure 2.3 models the sliding mass as a one-dimensional soil column. The seismic loadings for a rigid and flexible sliding masses are compared in Figure 2.4 for the GIL067 motion recorded during the 1989 Loma Prieta (M=6.9) earthquake. The acceleration time history for the rigid sliding mass has a larger intensity and displays significantly more high frequency

motion than the k-time history for the flexible sliding mass. Although the k-time history has a smaller intensity, the integration of the k-time history with respect to time (which produced a k-vel – time history, Rathje and Antonakos 2010) produces a time history that is very similar to the velocity time history for the rigid sliding mass. Both k_{max} and the maximum value of the k-vel – time history ($k\text{-}vel_{max}$) affect the level of sliding displacement.

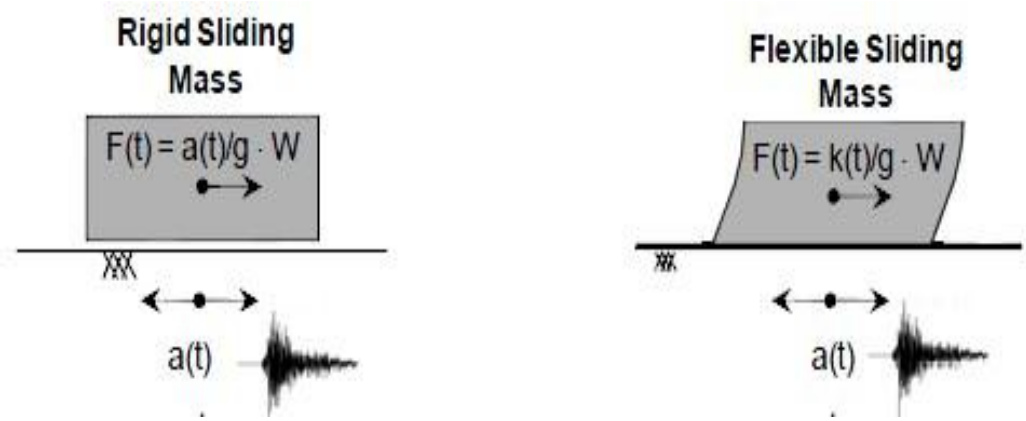

Figure 2.3 Comparison of Internal Deformation between Rigid Sliding Mass and Flexible Sliding Mass (Rathje and Antonakos 2010)

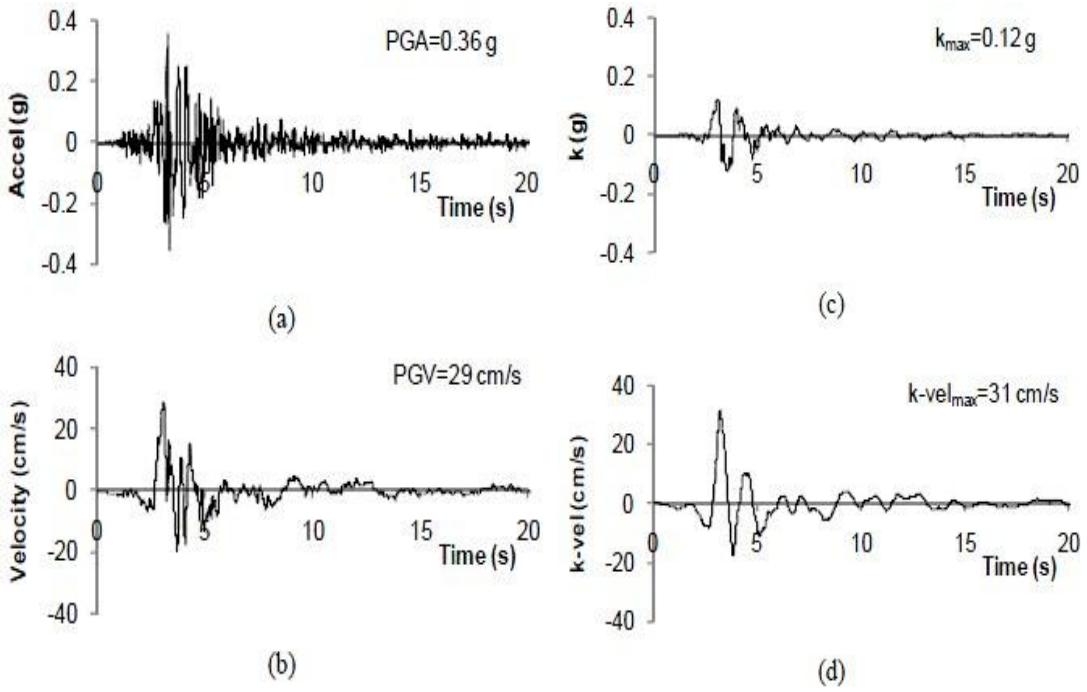

Figure 2.4 (a) Acceleration-time and (b) Velocity-time History for a Rigid Sliding Mass (c) k-time and (d) k-vel-time History for a Flexible Sliding Mass (Rathje and Antonakos 2010)

2.4 APPROACH TO SELECTING AND SCALING MOTIONS

For the sliding displacement analyses discussed above, acceleration-time histories are the input data required for the dynamic response and sliding displacement analyses. These motions must be selected to fit an appropriate level of ground shaking as defined by various ground motion parameters, such as Peak Ground Acceleration (PGA), Peak Ground Velocity (PGV), Arias Intensity (I_a) and the acceleration response spectrum. Most often, a target response spectrum is specified and motions selected and scaled to fit that target response spectrum. The target spectrum may be developed from

a ground motion prediction equation (GMPE) or from a Probabilistic Seismic Hazard Analysis (PSHA), and the target spectrum represents the expected ground shaking for a given earthquake even.

A suite of recorded acceleration-time histories (typically 5 to 15 motions) is commonly used for input into dynamic analyses, but these motions must be modified appropriately such that the median of the suite fits the target spectrum (Kramer 1996). The simplest approach to modifying acceleration-time histories is linearly scaling the motion based on a scale factor. Kottke and Rathje (2008) developed a semi-automated procedure for selecting and scaling recorded earthquake motions to fit a target spectrum.

Figure 2.5 displays a suite of acceleration-time histories selected and linearly scaled to fit a target spectrum. As shown in Figure 2.5, this suite of linearly scaled motions fits the target spectrum on average over all periods, but none of the motions within the suite fits the target spectrum exactly and some motions can be significantly different than the target spectrum.

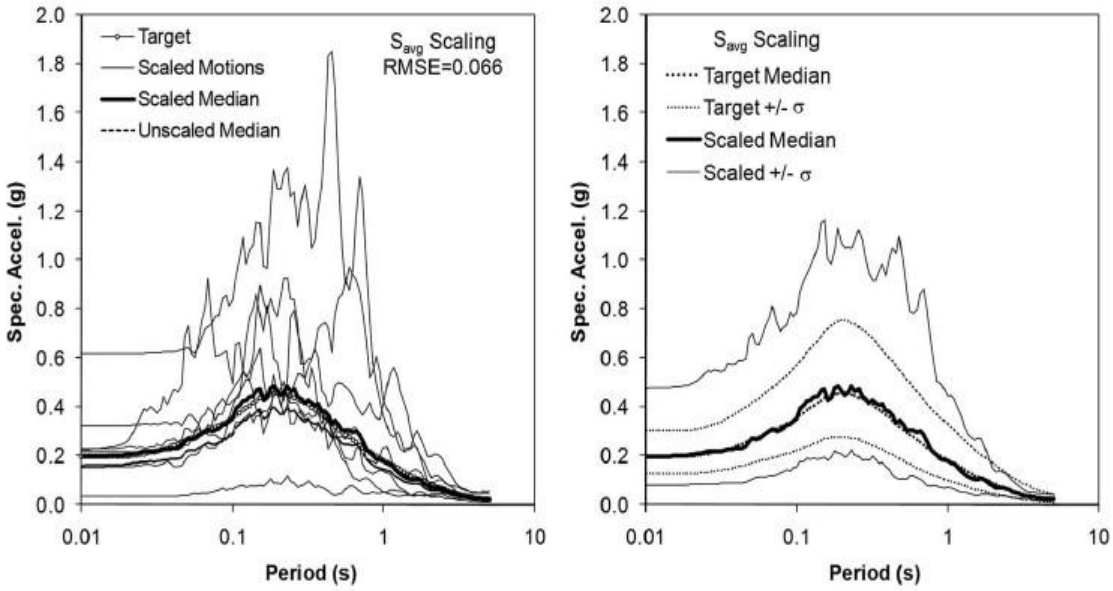

Figure 2.5 A Suite of Recorded Earthquake Motions Scaled to Fit the Target Response Spectrum (Kottke and Rathje, 2008)

Another approach for fitting a suite of ground motions to a target response spectrum is spectral matching, which modifies the frequency content of acceleration-time histories such that each motion fits the target response spectrum very closely. The program **RSPMatch** (Abrahamson, 1992; Hancock et al., 2006) was used to spectrally match selected ground motions to a target response spectrum. This program adds wavelets to the acceleration-time history in appropriate locations in an effort to modify the resulting acceleration response spectrum.

Figure 2.6 shows an original and adjusted time series spectrally matched using RSPMatch. Figure 2.7 shows the original and the spectrally matched response spectra, along with the target. After spectral matching, the acceleration response spectrum has

lost all its peaks and valleys such that it matched the target spectrum very well. However, the resulting response spectrum of the spectrally matched motion is not representative of an actual ground motion. .

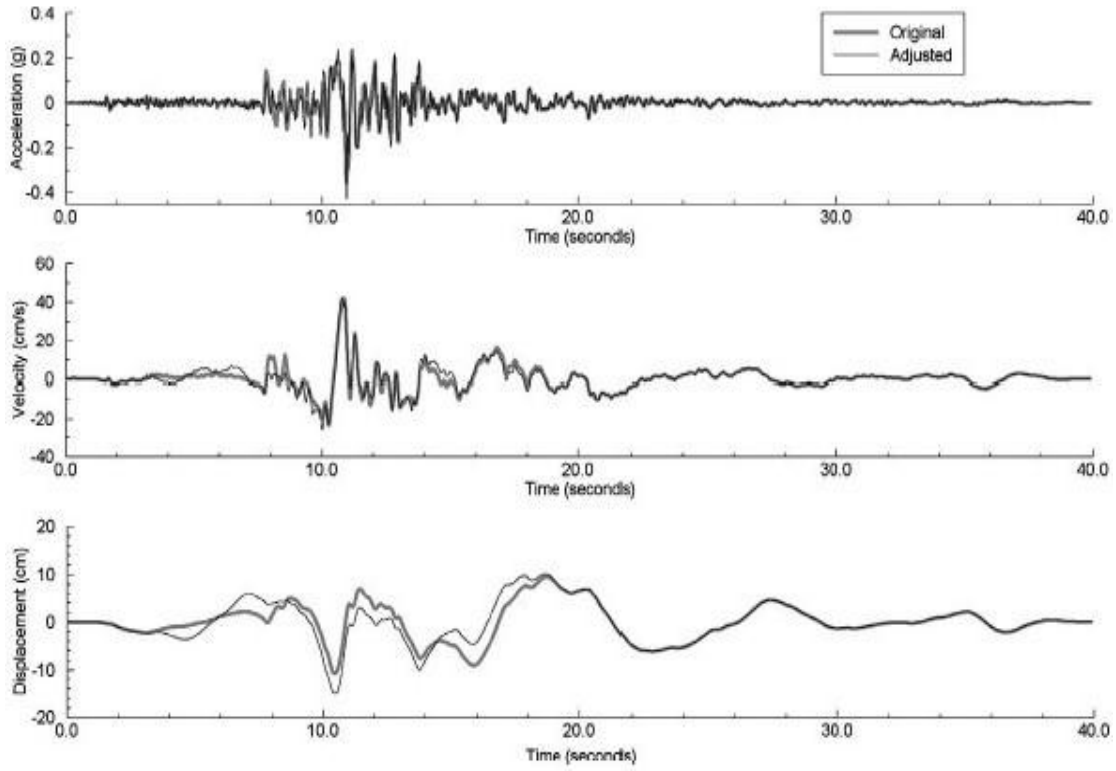

Figure 2.6 Comparison of the Acceleration, Velocity and Displacement Time Series of the Original Linearly Scaled Ground Motion (grey line) and Adjusted Ground Motion (black line) (from Hancock et al., 2006)

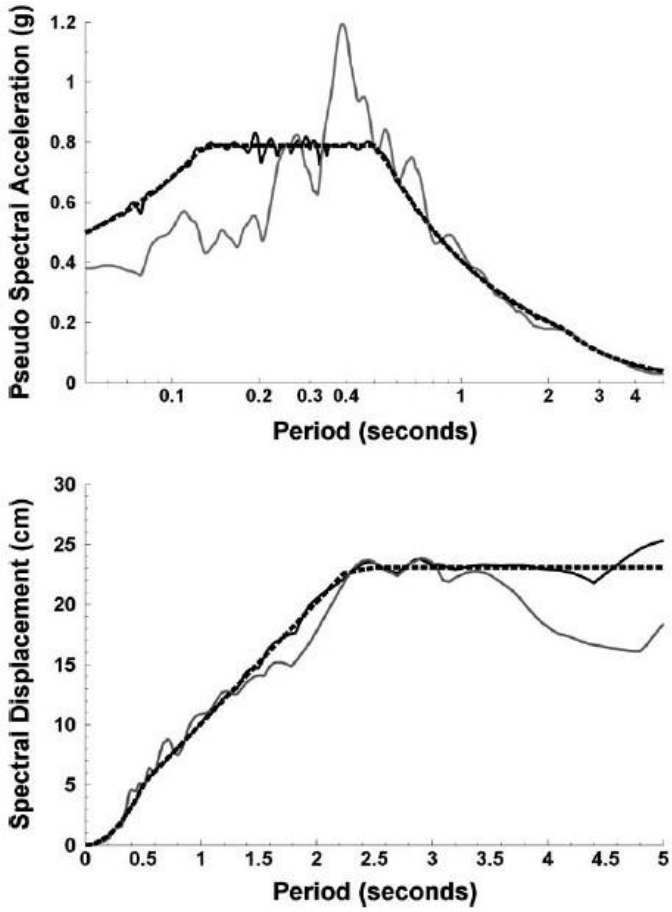

Figure 2.7 Spectral Acceleration (upper) and Spectral Displacement (lower) of the Target Response Spectrum (dashed black line), Original Linearly Scaled Motion (solid grey line) and Adjusted Ground Motion (solid black line) (from Hancock et al., 2006)

When performing sliding displacement analysis in practice, engineers have a choice to use linearly scaled input motions or spectrally matched input motions. However, it is not clear how the different motions will affect the computed sliding displacements.

2.5 EMPIRICAL PREDICTIVE MODELS

Compared with rigorous analyses for computing the sliding displacement, empirical predictive models are more simple and convenient to use. These empirical displacement models are based on statistical analysis of computed displacements for thousands of acceleration-time histories and different values of k_y. To use these empirical models, only ground motion parameters (e.g., PGA, PGV, etc.) are requires rather than full acceleration-time histories.

Saygili and Rathje (2008) developed a suite of empirical predictive models for computing the sliding displacement of slopes. Several ground motion parameters, such as Peak Ground Acceleration (PGA), Peak Ground Velocity (PGV), Mean Period (T_m, Rathje et al., 1998; Rathje et al., 2004) and Arias Intensity (I_a), are incorporated in these models. Rathje and Saygili (2009) modified their PGA model by adding a term related to Earthquake Magnitude (M). These models are appropriate for calculating rigid block sliding displacement.

The (PGA, PGV) rigid sliding block model was recommended by Saygili and Rathje (2008) and this model can be expressed as:

$$\ln D = -1.56 - 4.58\left(\frac{k_y}{PGA}\right) - 20.84\left(\frac{k_y}{PGA}\right)^2 + 44.75\left(\frac{k_y}{PGA}\right)^3 - 30.5\left(\frac{k_y}{PGA}\right)^4 - 0.64\ln(PGA) + 1.55\ln(PGV) + \varepsilon\sigma_{\ln D} \quad (2.1)$$

Where D=sliding displacement (cm); PGA=peak ground acceleration (g); PGV=peak ground velocity (cm/s); k_y = yield critical acceleration (g). To calculate the median sliding displacements, ε is set to 0.

Rathje and Antonakos (2010) extended the Saygili and Rathje (2008) models for flexible sliding conditions. This approach requires that the k_{max} be used rather than PGA, and that k-vel_{max} be used instead of PGV in the sliding displacement calculation. Rathje and Antonakos (2010) developed statistical models to predict k_{max} and k-vel_{max}, from the input PGA, PGV, and the period ratio (T_s/T_m). These expressions are shown in Figure 2.8 and are given by:

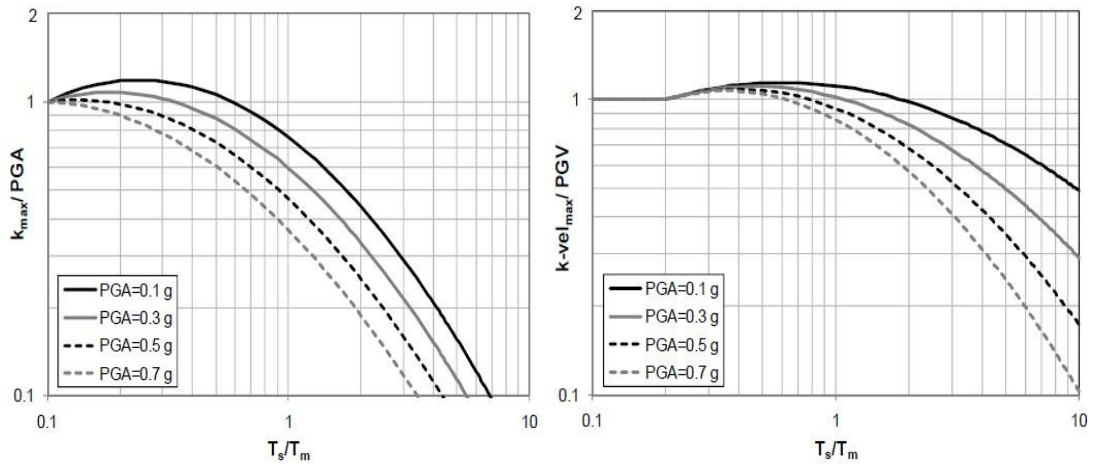

Figure 2.8 k_{max}/PGA Model Predictions and k-vel_{max}/PGV Model Predictions (Rathje and Antonakos 2010)

$$\ln(k_{max}/PGA) = (0.459 - 0.702 \cdot PGA) \cdot [\ln\left(\frac{T_S/T_m}{0.1}\right)] + (-0.228 + 0.07 \cdot PGA) \cdot [\ln\left(\frac{T_S/T_m}{0.1}\right)]^2 \quad \text{for } T_S/T_m \geq 0.1 \quad (2.2a)$$

$$\ln(k_{max}/PGA) = 0 \quad \text{for } T_S/T_m < 0.1 \quad (2.2b)$$

$$\ln(\text{k-vel}_{max}/PGV) = 0.240 \cdot [\ln\left(\frac{T_S/T_m}{0.2}\right)] + (-0.091 - 0.171 \cdot PGA) \cdot [\ln\left(\frac{T_S/T_m}{0.2}\right)]^2 \quad \text{for } T_S/T_m \geq 0.2 \quad (2.3a)$$

$$\ln(\text{k-vel}_{max}/PGV) = 0 \quad \text{for } T_S/T_m < 0.2 \quad (2.3b)$$

In addition to using k_{max} and k-vel_{max} in the Saygili and Rathje (2008) displacement model, an additional modification must be applied. This modification (Rathje and Antonakos 2010) can be expressed as:

$$\ln(D_{flexible}) = \ln(D_{PGA,PGV}) + 1.42T_S \quad \text{for } T_S \leq 0.5s \quad (2.4a)$$

$$\ln(D_{flexible}) = \ln(D_{PGA,PGV}) + 0.71 \quad \text{for } T_S > 0.5s \quad (2.4b)$$

Where $D_{PGA,PGV}$ represents the median sliding displacement predicted by the (PGA, PGV) rigid sliding block model (Saygili and Rathje 2008) and T_S is the natural period of the sliding mass. For the calculation of $D_{PGA,PGV}$, k_{max} and k-vel_{max} are used in lieu of PGA and PGV, respectively.

Chapter 3 Analyses Performed

3.1 INTRODUCTION

To compare the influence of ground motion scaling methods on the computed seismically-induced sliding displacements, six sliding masses with different configurations were subjected to a suite of linearly scaled input motions and a suite of spectrally matched input motions. Decoupled sliding displacement analyses were performed using an equivalent linear one-dimensional model of the sliding mass (Rathje and Bray 1999, Lee 2004). Sliding displacements from the different suites of input motions were compared for different values of k_y.

3.2 SITE INFORMATION

Five one-dimensional soil columns and one rigid sliding mass were analyzed. The heights and thicknesses of the soil columns (Table 3.1) were selected to represent a range of conditions and initial site periods. The site periods ($T_S = 4H/V_S$ where H is soil height and V_S is the shear wave velocity) range from 0.15s to 1.5s for the flexible sliding masses. The site period is 0.0s for the rigid sliding mass. Shear wave velocities are typical values for soil (250m/s ~ 400m/s). The depth of sites ranges from shallow (15m) to deep (100m). The shear wave velocity of bedrock beneath the soil deposit is $V_{s,rock} = 1000\text{m/s}$.

Table 3.1 Site Information

Site	H (m)	V_S (m/s)	T_S (s)
Rigid	0	N/A	0.0
A	15	400	0.15
B	30	400	0.3
C	30	250	0.48
D	100	400	1.0
E	100	265	1.51

These parameters were input into the software program named **SLAMMER** (developed by Jibson et al.) along with a k_y for sliding displacement analyses. Values of k_y equal to 0.05g and 0.1g are considered, as well as a lower bound of 0.01g. The analytical models used in the sliding displacement analyses in SLAMMER are discussed in Section 3.3.5.

3.3 INPUT GROUND MOTIONS

3.3.1 Scaled Motions to Fit Target Response Spectrum

In this study, a suite of 15 input ground motions was selected to fit a target acceleration spectrum for a magnitude (M_w) 6.5 earthquake at a distance (R) of 20 km based on the Boore and Atkinson (2008) Ground Motion Prediction Equation (GMPE). These motions were initially selected by Kottke and Rathje (2010) for a site response study. A semi-automated procedure (Kottke and Rathje 2008) was use to select and

scale the recorded ground motions. The selected motions are listed in Table 3.2.

Table 3.2 List of Selected Ground Motions from NGA Database

Record Names	Magnitude	Closest Distance (km)	$V_{S,30}$ (m/s)
CHICHI06-TCU076-E	7.62	2.76	615
ITALY-A-AUL270	6.90	9.55	1000
ITALY-A-BAG000	6.90	8.18	1000
ITALY-A-STU270	6.90	10.84	1000
ITALY-B-AUL270	6.20	29.86	1000
KOZANI-KOZ--L	6.40	19.54	659.6
LOMAP-G01000	6.93	9.64	1428
LOMAP-GIL067	6.93	9.96	729.7
MORGAN-GIL337	6.19	14.84	729.7
NORTHR-H12180	6.69	21.36	602.1
NORTHR-HOW330	6.69	16.88	821.7
NORTHR-LV1000	6.69	37.19	684.9
NORTHR-LV3090	6.69	37.33	684.9
NORTHR-WON185	6.69	20.30	1222.5
VICT-CPE045	6.33	14.37	659.6

As mentioned in Chapter 2, scaled motions are multiplied by linear scale factors to best fit the target response spectrum on average. The original target spectrum used by Kottke and Rathje (2010) had a Peak Ground Acceleration (PGA) of 0.13g. To represent a more common design level ground motion, the target response spectrum was scaled up to PGA=0.4g, and the entire suite of scaled motions scaled up accordingly. The distribution of the response spectra of the scaled motions are shown in Figure 3.1 along with the target response spectrum. The response spectra of the scaled

motions are widely distributed about the target spectrum over the entire period range.

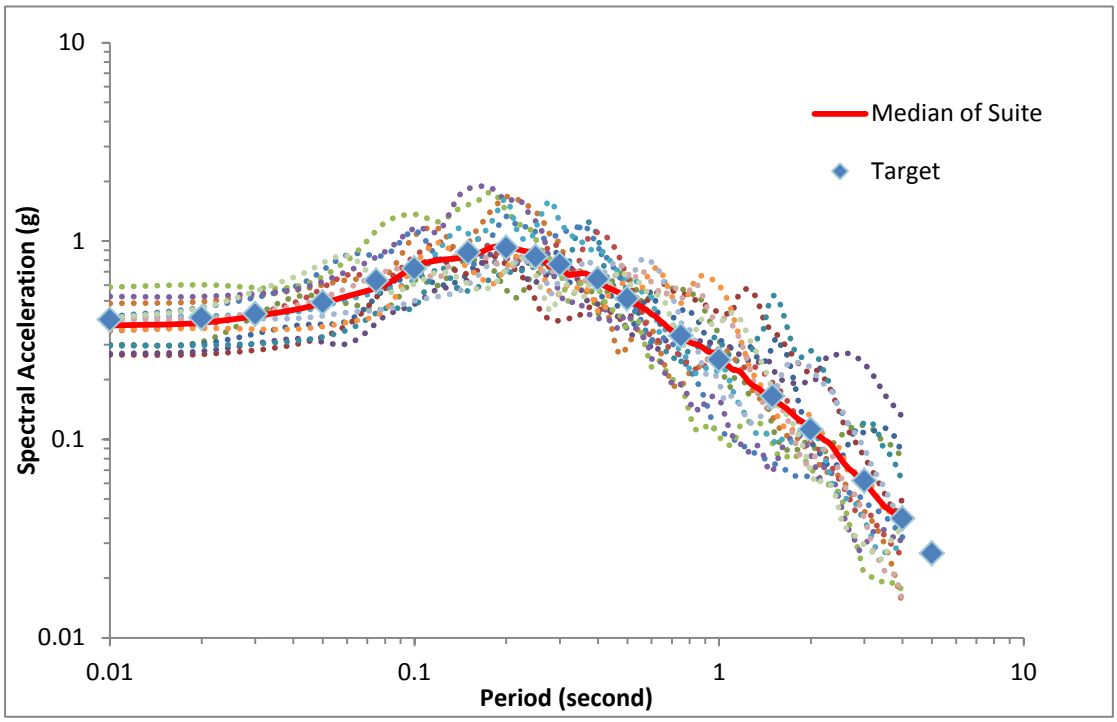

Figure 3.1 Response Spectra for Motions Scaled to Target Response Spectrum

3.3.2 Matched Motions to Fit Target Response Spectrum

The linearly scaled motions were spectrally matched to the target spectrum by Kottke and Rathje (2010) using the program **RSPMatch** (Abrahamson, 1992; Hancock, 2006).

The response spectra of the spectrally matched motions are shown in Figure 3.2 along with the target spectrum. In comparison to the scaled motions, all the spectrally

matched motions have a similar response spectrum to the target, except at periods less than about 0.1s.This difference occurs because the spectral matching process was only applied to the frequency range from 0.2 Hz to 25 Hz. As a result, the spectrally matched motions do not fit the target response spectrum well at period less than about 0.1s. In this period range, the spectrally matched motions are about 10% smaller than the target, on average.

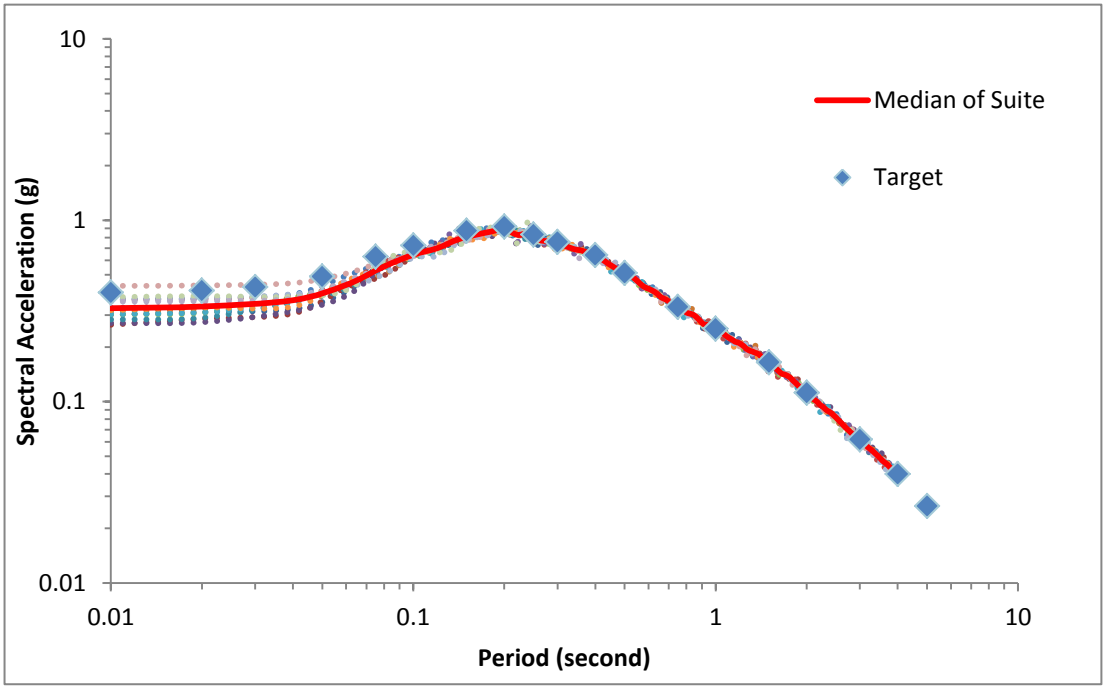

Figure 3.2 Response Spectra for Motions Matched to Target Response Spectrum

The median response spectra of the scaled motions and the spectrally matched motions are also compared with the target in Figure 3.3. Figure 3.3 illustrates that the median spectra of the two suites fit the target well, except for the spectrally matched

motions at periods less than 0.1s. In this period range, the spectrally matched motions are about 10% smaller, on average, than the scaled motions.

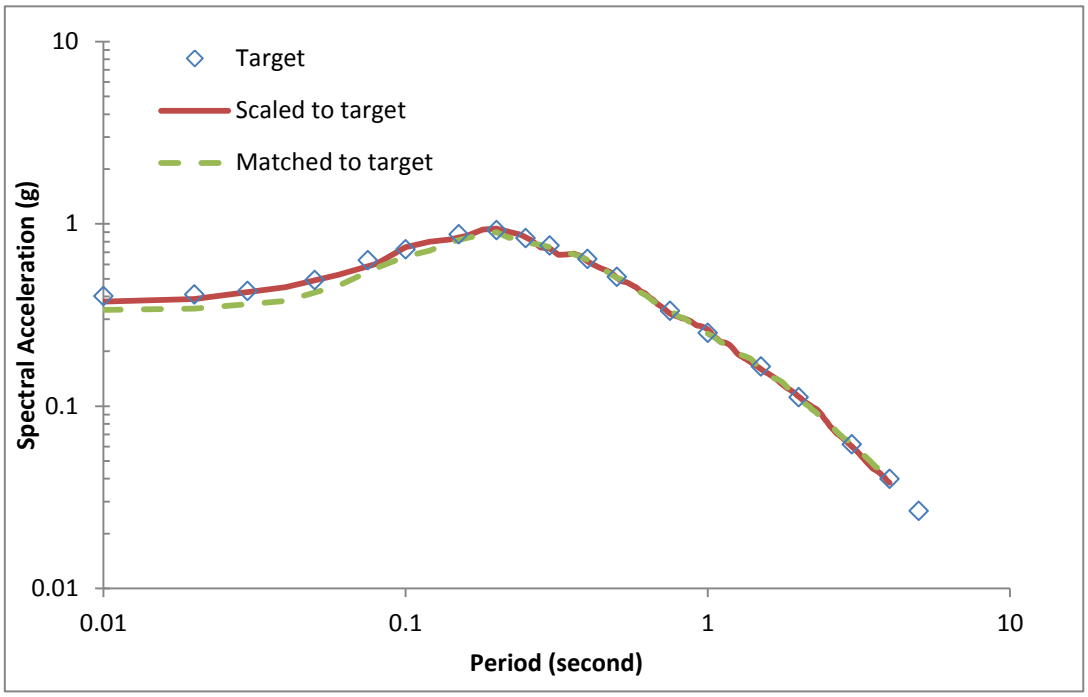

Figure 3.3 Median Response Spectra for Motions Scaled and Matched to Target Response Spectrum

The scaled and matched ground motion records are listed in Table 3.3, along with their corresponding PGA, Peak Ground Velocity (PGV) and Mean Period (T_m). The median ground motion parameters for each suite and their standard deviation are also listed in Table 3.3. For a single motion, the spectral matching process can change a ground motion parameter (i.e. PGA, PGV or T_m) by as much as a factor of 2.0 (e.g. PGV values of ITALY-A-STU270). However, the median PGA, PGV and T_m values for the two suites are more similar.

The median PGA of the scaled motions is about 11% higher than the spectrally matched motions. The median PGV of the scaled motions is about 14% higher than the spectrally matched motions. The median T_m of the scaled motions is about 13% higher than the spectrally matched motions. Basically, the scaled suite displays median ground motion parameters that are 11% to 14% larger than the spectrally matched suite.

Table 3.3 Ground Motion Parameters for Motions Scaled and Matched to Target Response Spectrum

	PGA (g)		PGV (cm/s)		T_m (s)	
Earthquake Records	Scaled	Matched	Scaled	Matched	Scaled	Matched
CHICHI06-TCU076-E	0.301	0.307	27.7	21.7	0.50	0.41
ITALY-A-AUL270	0.298	0.299	29.1	23.1	0.49	0.42
ITALY-A-BAG000	0.267	0.272	42.3	23.1	0.67	0.43
ITALY-A-STU270	0.27	0.291	39.2	22.3	0.86	0.48
ITALY-B-AUL270	0.297	0.325	29.9	20.9	0.66	0.46
KOZANI-KOZ--L	0.485	0.368	21.1	27.1	0.28	0.32
LOMAP-G01000	0.417	0.367	32.0	28.8	0.29	0.34
LOMAP-GIL067	0.352	0.309	28.2	25.5	0.37	0.36
MORGAN-GIL337	0.586	0.342	17.7	23.3	0.22	0.31
NORTHR-H12180	0.525	0.312	18.1	26.4	0.22	0.29
NORTHR-HOW330	0.416	0.324	21.6	22.9	0.32	0.35
NORTHR-LV1000	0.356	0.383	31.2	23.8	0.50	0.40
NORTHR-LV3090	0.404	0.449	30.8	22.6	0.54	0.45
NORTHR-WON185	0.402	0.378	27.6	25.0	0.46	0.36
VICT-CPE045	0.409	0.372	20.8	19.0	0.51	0.41
Median	**0.375**	**0.337**	**27.0**	**23.6**	**0.43**	**0.38**
σ_{ln}	0.240	0.132	0.260	0.106	0.410	0.153

As expected, the standard deviation of the spectrally matched motions is

smaller than the standard deviation of the scaled motions for PGA, PGV and T_m.

3.3.3 Matched Motions to Fit Target Response Spectrum and Peak Ground Velocity

PGV significantly affects the computed sliding displacements of slopes (Saygili and Rathje 2008). The suite of spectrally matched motions has a smaller median PGV value than the suite of scaled motions, which will affect the comparison of computed displacements. Therefore, the spectrally matched motions were further scaled, so that their median PGV would be equal to the median PGV of the scaled motions. This scale factor was based on the median PGV values of the two suites and is equal to:

$$\text{Scale factor} = \frac{\text{median PGV}_{\text{scaled}}}{\text{median PGV}_{\text{matched}}} = \frac{27.0\text{cm/s}}{23.6\text{cm/s}} \cong 1.14 \qquad (3.1)$$

This scale factor was applied to each spectrally matched motion. Therefore, the PGA and PGV values of each spectrally matched motion were scaled up by a factor 1.14. As a result, the scaled motions and spectrally matched motions have nearly the same median PGV (and PGA, Table 3.4). However, the median T_m value did not change due to the scaling, because the linear scaling process does not change the frequency content of an acceleration-time history.

The standard deviations for PGA and PGV are not changed by this further

scaling because a constant scale factor was applied to all motions.

As seen in Figure 3.4, the median response spectra of scaled and spectrally matched motions now fit very well in the short period range. However, there are now some differences at longer periods.

Table 3.4 Ground Motion Parameters for Motions Scaled and Matched to Target Response Spectrum and PGV

	PGA (g)		PGV (cm/s)		T_m (s)	
Earthquake Records	Scaled	Matched	Scaled	Matched	Scaled	Matched
CHICHI06-TCU076-E	0.301	0.350	27.7	24.7	0.50	0.41
ITALY-A-AUL270	0.298	0.341	29.1	26.3	0.49	0.42
ITALY-A-BAG000	0.267	0.310	42.3	26.3	0.67	0.43
ITALY-A-STU270	0.27	0.332	39.2	25.4	0.86	0.48
ITALY-B-AUL270	0.297	0.371	29.9	23.8	0.66	0.46
KOZANI-KOZ--L	0.485	0.420	21.1	30.9	0.28	0.32
LOMAP-G01000	0.417	0.418	32.0	32.8	0.29	0.34
LOMAP-GIL067	0.352	0.352	28.2	29.1	0.37	0.36
MORGAN-GIL337	0.586	0.390	17.7	26.6	0.22	0.31
NORTHR-H12180	0.525	0.356	18.1	30.1	0.22	0.29
NORTHR-HOW330	0.416	0.369	21.6	26.1	0.32	0.35
NORTHR-LV1000	0.356	0.437	31.2	27.1	0.50	0.40
NORTHR-LV3090	0.404	0.512	30.8	25.8	0.54	0.45
NORTHR-WON185	0.402	0.431	27.6	28.5	0.46	0.36
VICT-CPE045	0.409	0.424	20.8	21.7	0.51	0.41
Median	**0.375**	**0.384**	**27.0**	**26.9**	**0.43**	**0.38**
σ_{ln}	0.240	0.132	0.260	0.106	0.410	0.153

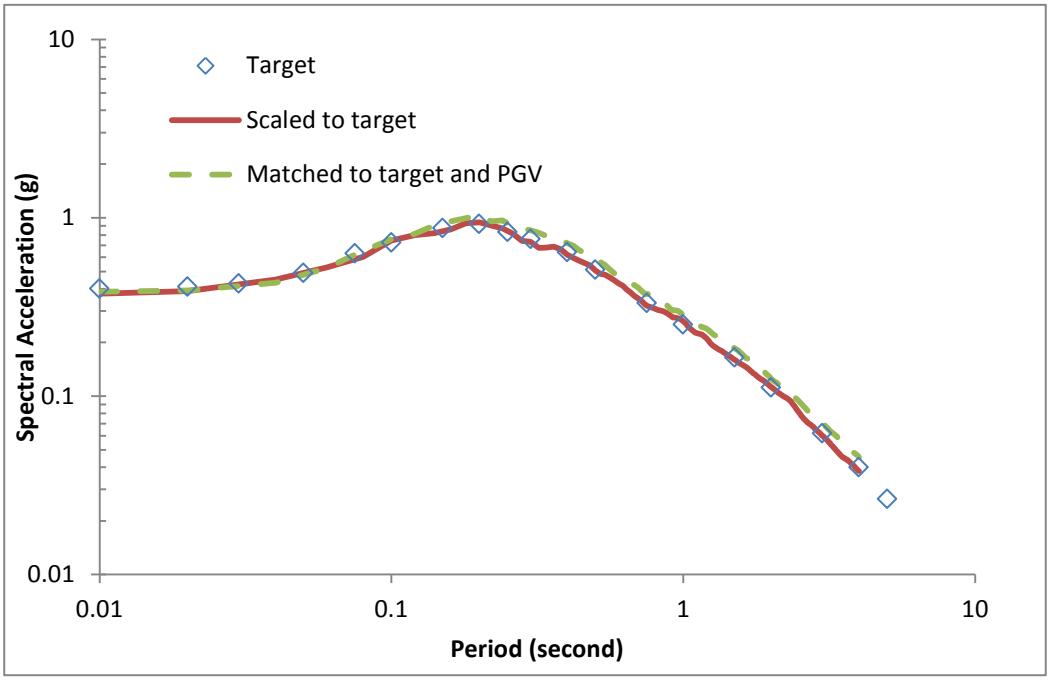

Figure 3.4 Median Response Spectra for Motions Scaled and Matched to Target Response Spectrum and PGV

3.3.4 Scaled Motions to Target Response Spectrum at Site Period

Some engineers may focus scaling their motions to fit the target response spectrum exactly at the period of the site being analyzed. This scaling method attempts to ensure that the intensity of the motion in the period range close to T_s is captured well. However, this approach does not consider that other frequencies also affect the dynamic and sliding responses.

To investigate this scaling method, the suite of scaled motions was further scaled to fit the spectral acceleration at $T_s = 1.0s$ (i.e. the site period for Site D). For

the target response spectrum, S_a is equal to 0.252g at site period 1.0s. The response spectra of the motions after scaling all the selected ground motions to 0.252g at $T_s = 1.0s$, are shown in Figure 3.5. The resulting PGA, PGV and Scale factor values of these scaled motions are listed in Table 3.5. Note that the median response spectrum still matches the target well (Figure 3.5 and Figure 3.6). Because the median response spectrum of these scaled motions was already very close to the target response spectrum before this further scaling process, the median response spectrum of the new suite is only slightly lower than the former one (Figure 3.6).

The scale factor varies in a wide range, which is from 0.42 to 2.43. So most motions were changed significantly after scaling to 0.252g at $T_s = 1.0s$. However, the median PGA and PGV values were only changed slightly. However the variability is significant at periods away from $T_S = 1.0s$. To better show the changes in variability across the entire period range, the standard deviation of the natural logarithm of the spectral accelerations at each period are shown in Figure 3.7. For comparison, the standard deviations for the originally scaled motion and the spectrally matched motions are also shown. The standard deviation of the spectral accelerations for the suite scaled to Sa = 0.252 g at T = 1.0 s is zero at T = 1.0 s, and in the period range from 0.7s to 1.6s it is smaller than for the originally scaled motions. However, the standard deviation becomes much larger in the other period range.

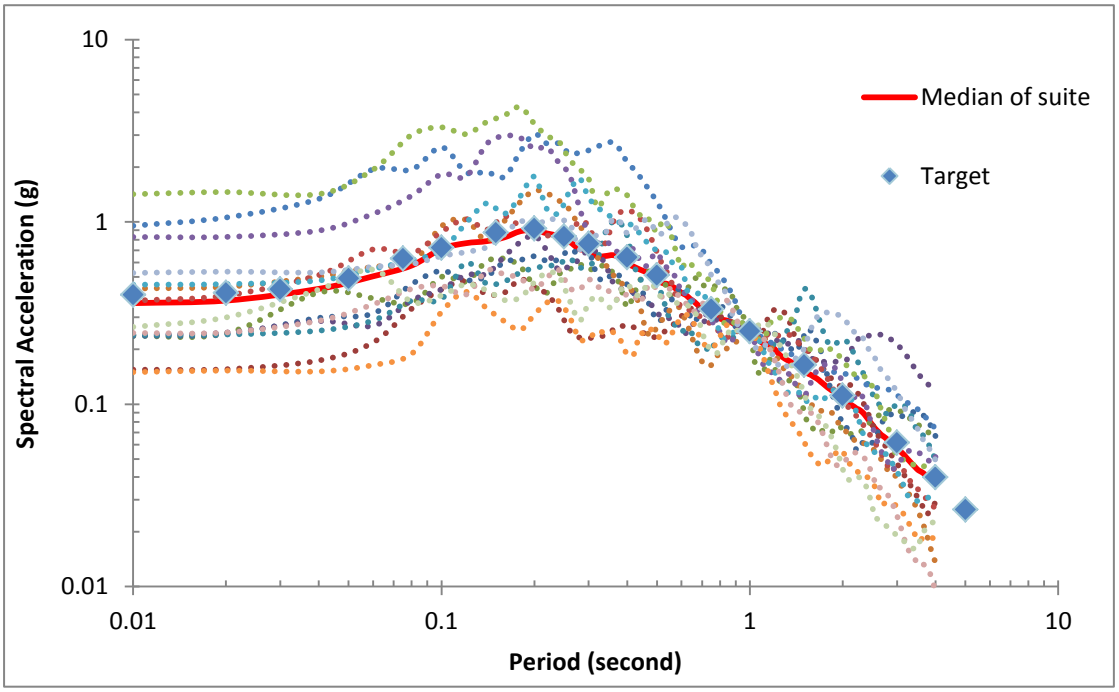

Figure 3.5 Response Spectra for Motions Scaled to Target Response Spectrum at T_S=1.0s

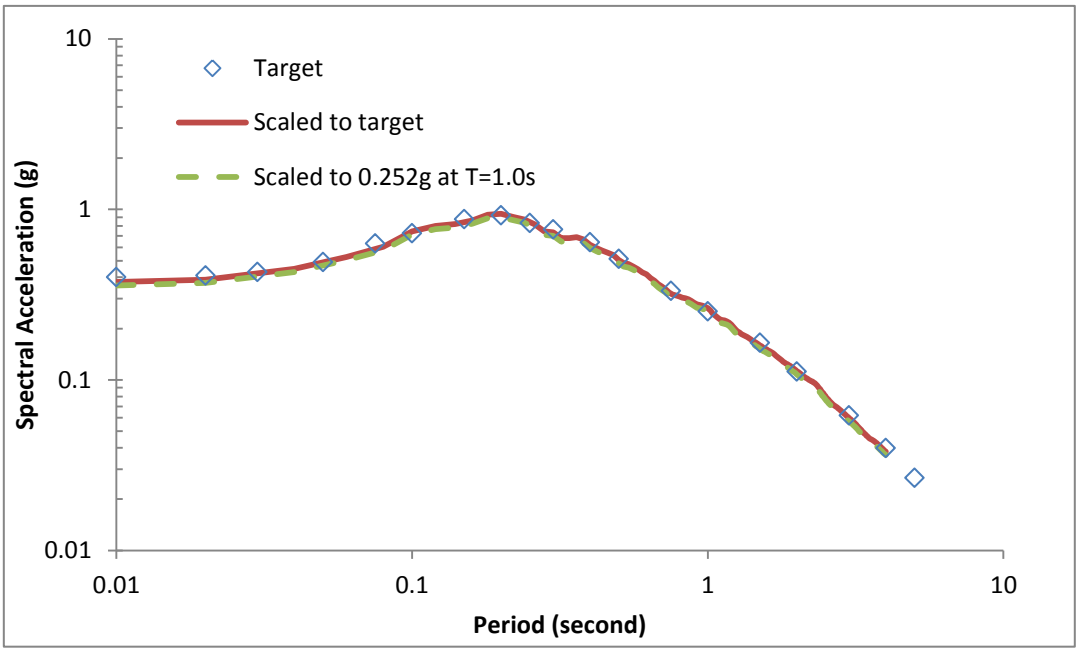

Figure 3.6 Median Response Spectra for Motions Scaled to Target Response Spectrum at T_S=1.0s and Scaled to Target Response Spectrum

Table 3.5 Ground Motion Parameters for Motions Scaled to Target Response Spectrum at T_S=1.0s and Motions Scaled to Target Response Spectrum

Earthquake Records	PGA (g)		PGV (cm/s)		Scale factor (Scaled at T=1.0s/Scaled to target)
	Scaled to target	Scaled at T=1.0s	Scaled to target	Scaled at T=1.0s	
CHICHI06-TCU076-E	0.301	0.237	27.7	21.8	0.79
ITALY-A-AUL270	0.298	0.238	29.1	23.2	0.80
ITALY-A-BAG000	0.267	0.155	42.3	24.5	0.58
ITALY-A-STU270	0.270	0.240	39.2	34.8	0.89
ITALY-B-AUL270	0.297	0.241	29.9	24.2	0.81
KOZANI-KOZ--L	0.485	0.432	21.1	18.8	0.89
LOMAP-G01000	0.417	0.954	32.0	73.2	2.29
LOMAP-GIL067	0.352	0.370	28.2	29.6	1.05
MORGAN-GIL337	0.586	1.421	17.7	42.9	2.43
NORTHR-H12180	0.525	0.828	18.1	28.5	1.58
NORTHR-HOW330	0.416	0.454	21.6	23.6	1.09
NORTHR-LV1000	0.356	0.150	31.2	13.1	0.42
NORTHR-LV3090	0.404	0.525	30.8	40.0	1.30
NORTHR-WON185	0.402	0.246	27.6	16.9	0.61
VICT-CPE045	0.409	0.266	20.8	13.5	0.65
Median	**0.375**	**0.359**	**27.0**	**25.8**	**0.96**
$\boldsymbol{\sigma_{ln}}$	0.240	0.663	0.260	0.452	0.491

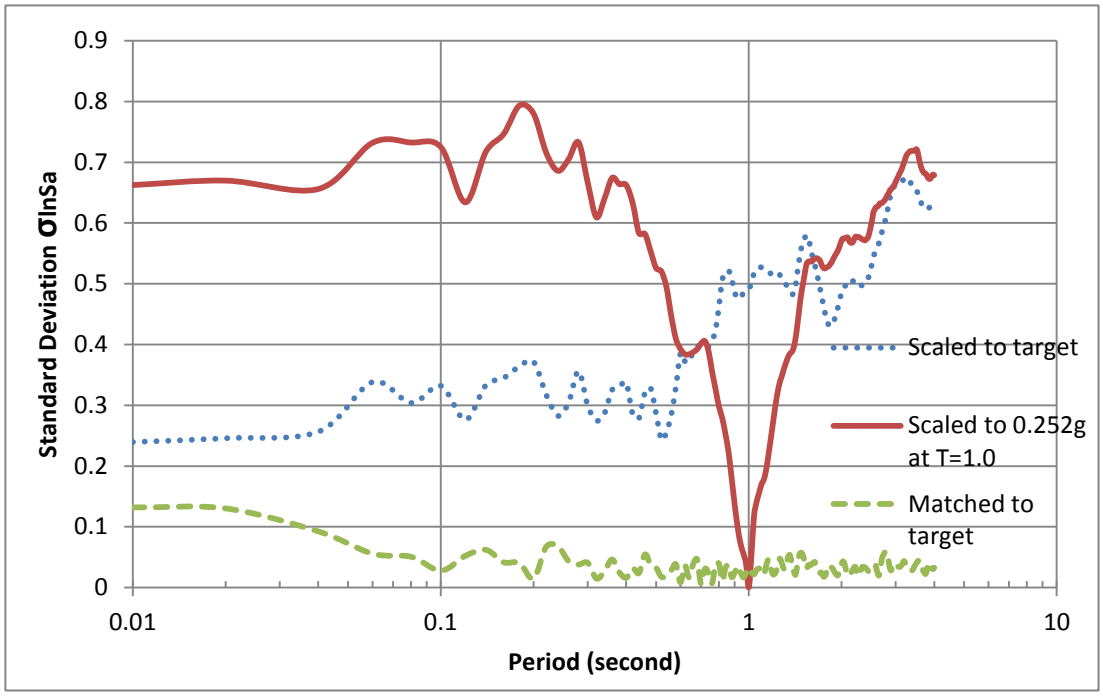

Figure 3.7 The Standard Deviation of the Natural Logarithmic of the Spectral Acceleration

3.3.5 Model for Sliding Displacement Analysis

A simplified one-dimensional, single degree of freedom (SDOF) system is used to represent the dynamic response of the earth structure (Rathje and Bray 1999). This SDOF model uses a mode shape appropriate for a horizontal soil deposit. The displacement profile within this sliding mass can be expressed as:

$$u(y,t) = \phi_1(y)Y_1(t) \qquad (3.2)$$

Where:

$u(y,t)$ = displacement at depth y and time t,
$\phi_1(y)$ = fundamental mode shape and
$Y_1(t)$ = modal coordiante (displacement at ground surface)

The mode shape for a horizontal soil deposit used in this model was developed by Idriss and Seed (1968) and is shown in Figure 3.8.

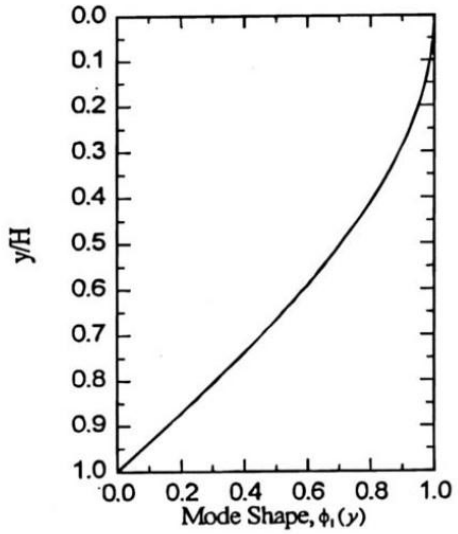

Figure 3.8 Model Used in this Study (from Rathje and Bray 1999)

Because of nonlinear soil behavior, using linear elastic material properties to evaluate the dynamic response of a soil deposit during an earthquake is not appropriate. The reduction in shear modulus and increase in material damping ratio with increasing shear strain are the essential nonlinear characteristics to model. To approximate the nonlinear response of a soil deposit with linear elastic analysis, the equivalent linear approach is used. The equivalent linear approach uses strain dependent dynamic properties that are selected based on an iterative procedure. is performed in the program SLAMMER. For this approach, the shear strains induced in the soil mass must

be computed for use in selecting the strain-compatible soil properties. The shear strain profile induced in the modal model is the derivative of the displacement profile shown in Figure 3.8, with the maximum shear strain induced at the bottom of the soil deposit. The shear strain used to select the strain-compatible soil properties in this modal model is taken as the value in the middle of the soil deposit (Lee, 2004). This approach is implemented in SLAMMER, along with nonlinear modulus reduction and damping curves for a Plastic Index=30 soil (Stokoe and Darendeli 2001). Additionally, only down-slope displacement is considered, because the up-slope yield critical acceleration is significantly larger than the down-slopek_y. There are two polarities of displacements, one induced by positive accelerations and the other one induced by negative accelerations. The average displacement of those two polarities is used in the following comparisons, because earthquakes can impact slopes in any direction.

Chapter 4 Comparisons of Sliding Displacements

4.1 INTRODUCTION

Sliding displacements were calculated for each suite of scaled and spectrally matched input motions described in Chapter 3 (i.e., fit to target spectrum, fit to target spectrum and PGV, fit to the spectral acceleration at the site period) for three different values of yield acceleration. Rigid sliding block displacements were calculated as well as decoupled displacements for the five deformable sliding masses. Comparisons are made between the median displacement for each suite of ground motions and the parameters influencing ant differences are investigated.

4.2 SCALED AND MATCHED MOTIONS TO FIT TARGET RESPONSE SPECTRUM

Sliding displacements were computed for the rigid sliding mass and five flexible sliding masses described in Section 3.1. Initially, a k_y equal to 0.05g was used. Figure 4.1 shows the computed sliding displacements for the scaled and spectrally matched motions individually for each site, along with the median displacement. On average, the median displacement for the scaled motions is larger than the median for the spectrally matched motions. This difference is most significant for Site E ($T_S = 1.51s$).

The displacement distributions of the scaled motions are wider than those of

spectrally matched motions, because the individual scaled motions have more variability between them. The standard deviation of the natural logarithm of the computed displacements is presented in Table 4.1 to quantify the variability in displacements. For comparison, Figure 4.2 shows the spectral acceleration S_a at each site period for the two suites of motions, and Table 4.2 lists the standard deviation of S_a in natural logarithmic units for the two suites. At $T_S \leq 0.15s$, the variability in the displacements from the spectrally matched motions is about 15% less than from the scaled motions, while it is 50% to 80% less for $T_S = 0.3s$ to 1.0s. These differences are directly related to the differences in σ_{lnSa} at the natural period of each site (Figure 4.2 and Table 4.2). At $T_S = 1.51s$, the standard deviations for displacement are similar and quite large for the scaled and spectrally matched motions. Here, because of the long site period, k_{max} is very small and becomes close to the k_y used in this analysis. As k_{max} approaches k_y, the variability σ_{lnD} is very large (Saygili and Rathje 2008, Rathje and Antonakos 2010). Note that the displacements for this case are very small (Figure 4.1).

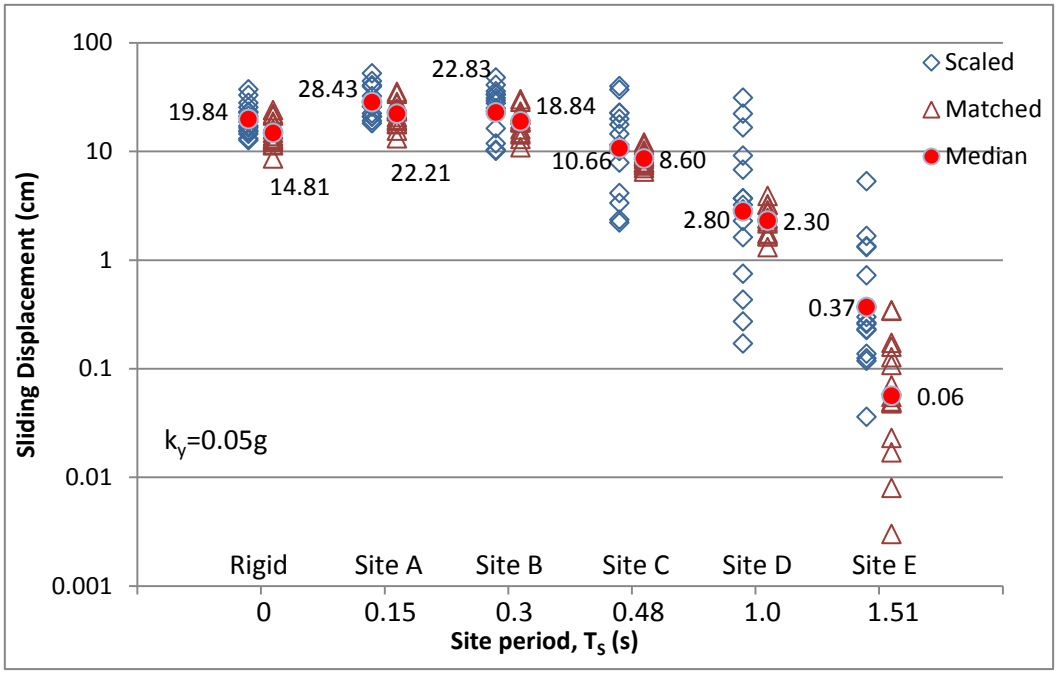

Figure 4.1 The Displacement Distribution of Motions Scaled and Matched to Target Response Spectrum (k_y=0.05g)

Table 4.1 Standard Deviation of Natural Logarithm of Displacements of Motions Scaled and Matched to Target Response Spectrum (k_y=0.05g)

	Rigid		Site A		Site B		Site C		Site D		Site E	
	S	M	S	M	S	M	S	M	S	M	S	M
σ_{lnD}	0.332	0.287	0.322	0.275	0.539	0.283	0.935	0.174	1.570	0.305	1.274	1.328

S: scaled motion **M**: matched motion

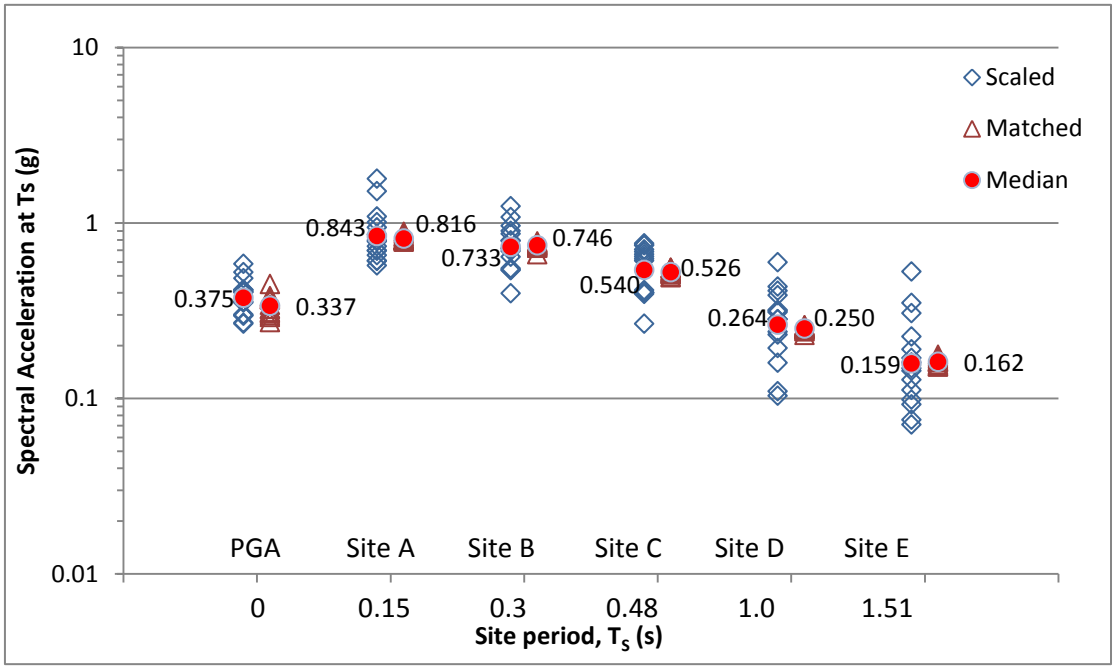

Figure 4.2 The Spectral Acceleration Distribution of Motions Scaled and Matched to Target Response Spectrum at Each Site Period, T_S

Table 4.2 Standard Deviation of Natural Logarithm of Spectral Acceleration of Motions Scaled and Matched to Target Response Spectrum at Each Site Period, T_S

	PGA		Site A		Site B		Site C		Site D		Site E	
	S	M	S	M	S	M	S	M	S	M	S	M
σ_{lnSa}	0.240	0.132	0.332	0.037	0.300	0.041	0.328	0.038	0.491	0.032	0.571	0.046

S: scaled motion **M**: matched motion

A displacement ratio is defined for comparing the relative displacement amplitudes between the scaled motions and spectrally matched motions.

$$\text{Displacement Ratio} = \frac{\text{computed displacement of a spectrally matched motion}}{\text{computed displacement of a scaled motion}} \qquad (4.1)$$

The displacement ratio is calculated for each spectrally matched motion and its corresponding scaled motion. Figure 4.3 shows the distribution of the displacement ratios for each site. The data show that the median displacement ratio is between 0.75 and 0.83 for site periods less than or equal to 1.0s, indicating that the displacements of the spectrally matched motions are about 20% smaller than the displacements of the scaled motions, on average. This ratio falls to 0.15 for $T_S = 1.51s$. To assess what is causing this difference, the ground motion characteristics of the scaled and spectrally matched motions are considered.

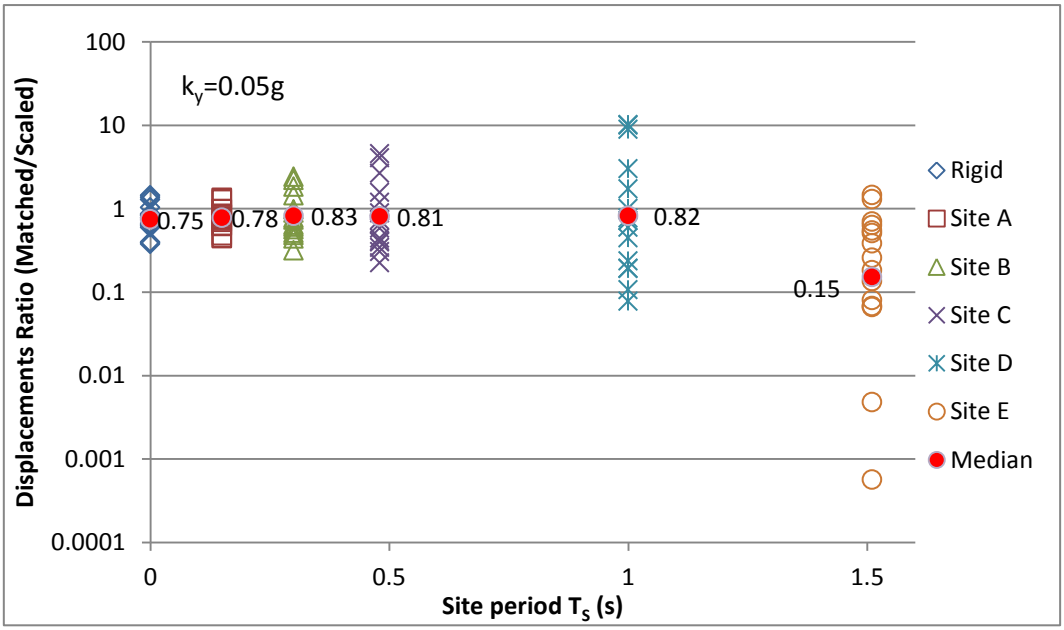

Figure 4.3 Displacement Ratios of Motions Scaled and Matched to Target Response Spectrum for Each Site (k_y=0.05g)

The ratio of median response spectra of the suite of spectrally matched and the

suite of scaled motions is shown in Figure 4.4, over the periods represented by the sites in this study. The median S_a ratio is between 0.85 and 1.0 in the short-period range (T<0.25s), and varies around 1.0 in the longer period range (T>0.25s). The difference in median spectral acceleration is somewhat consistent with the displacement ratio (i.e. matched/scaled < 1.0), but only at shorter periods. An additional consideration is that the PGV of the spectrally matched motions are about 13% smaller than the scaled motions (Table 3.3)

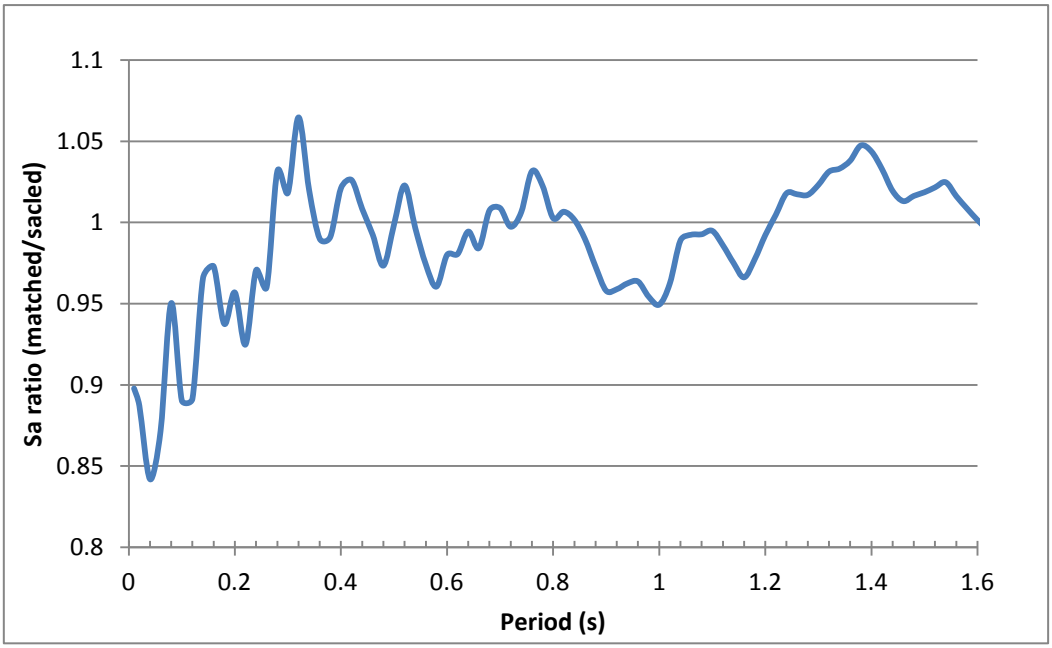

Figure 4.4 Median S_a Ratio of Motions Scaled and Matched to Target Response Spectrum

Considering the effect of these ground motion characteristics, the relationship between the displacement ratio and the ground motion ratio of each input motion is

investigated. The ground motion ratio is defined as the ground motion parameter of each spectrally matched motion divided by the same ground motion parameter of its corresponding scaled motion. Ground motion parameters PGA, PGV, and S_a at T_S are considered. Figure 4.5 plots the displacement ratio versus these various ground motion ratios for the six sites considered.

For the rigid site (Figure 4.5a), there is a negative correlation between the PGA ratio and displacement ratio (i.e., ground motions with a larger PGA have smaller displacements), which indicates that ground motion parameters beyond PGA are affecting the computed sliding displacement. A ground motion with a higher PGA may not have larger accelerations on average over the whole time domain, such that it does not produce a larger displacement. From Figure 4.5a, the PGV ratio and displacement ratio are highly correlated for the rigid condition. PGV provides information about the intensity of ground acceleration as well as frequency content because velocity is the integral of acceleration with respect to time, and thus significantly influences the level of sliding displacement. Saygili and Rathje (2008) demonstrated the strong relationship between PGV and sliding displacement. The results in Figure 4.5a suggest that the smaller values of PGV for the spectrally matched motions are causing the smaller average displacement from the spectrally matched motions.

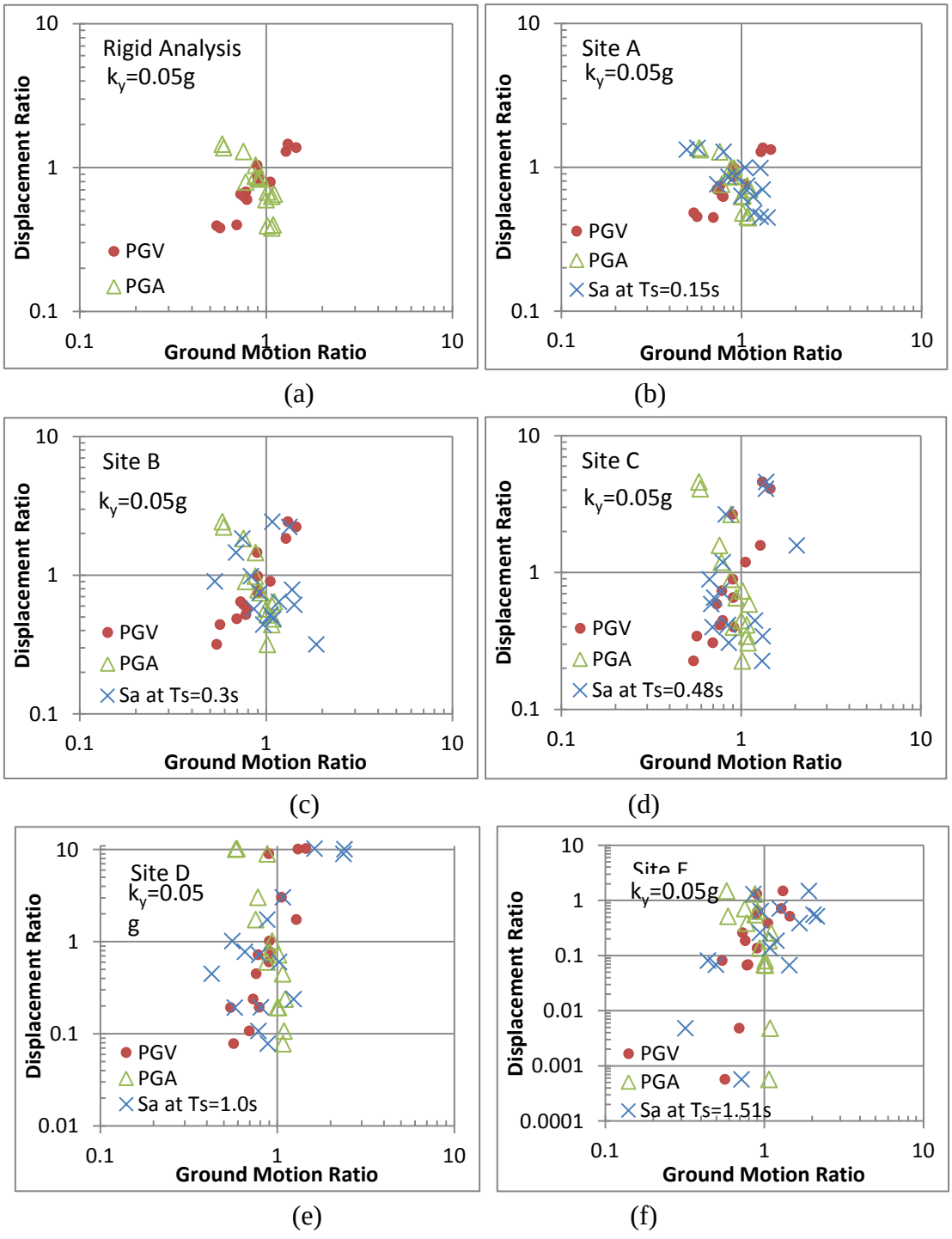

Figure 4.5 Ground Motion Ratios (matched/scaled) vs. Displacement Ratio (matched/scaled) for Motions Scaled and Matched to Target Response Spectrum for (a) Rigid, (b) Site A, (c) Site B, (d) Site C, (e) Site D, (f) Site E (k_y=0.05g)

For the flexible sites with $T_S \leq 1.0s$ (Figure 4.5b to 4.5e), the PGV of the input motion correlates better with the displacement than either PGA or S_a at the site period. These data appear to indicate that the differences between the displacements computed with the scaled and spectrally matched motions are being controlled by differences in the PGV. However, displacements for the flexible sites are computed from the k-time history, which represents the dynamic response of the sliding, rather than from the input acceleration-time history. Thus, it is also important to also consider the ground motion characteristics of the k-time history.

The important characteristics of a k-time history are k_{max} (i.e. maximum value in k-time history) and k-vel_{max} (i.e., maximum of velocity time history computed from k-time history) as described by Rathje and Antonakos (2010). Unfortunately, SLAMMER does not report the computed k-time history or k_{max} for an input ground motion. However, the statistical models of Rathje and Antonakos (2010) can be used to estimate k_{max} and k-vel_{max} for motions considered. The Rathje and Antonakos (2010) model was described in Section 2.4 and predicts k_{max} and k-vel_{max} as a function of input PGA, input PGV, input T_m, and T_S. Using the median values of PGA, PGV, and T_m of the suite of scaled motions (i.e. PGA = 0.375, PGV = 27 cm/s, T_m = 0.43 s) and the suite of spectrally matched motions (i.e. PGA = 0.337, PGV = 23.6 cm/s, T_m = 0.38 s), the median values of k_{max} and k-vel_{max} were predicted and are reported in Table 4.3. For the input motions the median PGA ratio is 0.91 and the

median PGV ratio is 0.87. The dynamic response of the sliding masses generally results in k_{max} ratios (analogous to the PGA ratio for rigid sliding) less than 0.91 and k-vel_{max} ratios (analogous to the PGV ratio for rigid sliding) less than 0.87. Thus, the dynamic responses of the sliding masses increase the differences in the ground motion characteristics. These smaller k_{max} and k-vel_{max} values for the spectrally matched motions are the result predominantly in their smaller T_m values, which lead to a diminished response. As a result of this diminished response, the spectrally matched motions produce less displacement.

Table 4.3 Predicted Dynamic Response Parameters Using Rathje and Antonakos (2010) Model for Motions Scaled to Target Response Spectrum

Site Period (s)	k_{max} (g)			k-vel_{max} (cm)		
	Matched	Scaled	Ratio	Matched	Scaled	Ratio
0.15	0.312	0.350	0.90	25.9	29.4	0.87
0.3	0.224	0.258	0.89	24.8	28.6	0.88
0.48	0.161	0.188	0.87	22.2	25.8	0.87
1.0	0.080	0.096	0.86	16.4	19.2	0.86
1.51	0.049	0.060	0.83	12.9	15.1	0.85

The data for Site E ($T_S = 1.51s$, Figure 4.5f) is very scattered because this long period site produces small values of k_{max} that happen to be close to the k_y of 0.05 g (see Table 4.3). For this site, 13 of the 15 motions have the displacement from the matched motion less than from the corresponding scaled motion (Table 4.4). In

particular, two spectrally matched motions (ITALY-A-STU270 and ITALY-B-AUL270) have extremely small displacements and their corresponding scaled motions have large displacements, which significantly draw down the ratio of median displacement. Figure 4.6 shows that the acceleration response spectra of these two scaled motions are much higher than the median response spectrum at periods greater than 1.0s, which leads to the very large displacements for the scaled motions. Additionally, the PGV values for these scaled motions are much larger than for the spectrally matched motions (Table 3.3), which contribute to the larger displacements for these scaled motions.

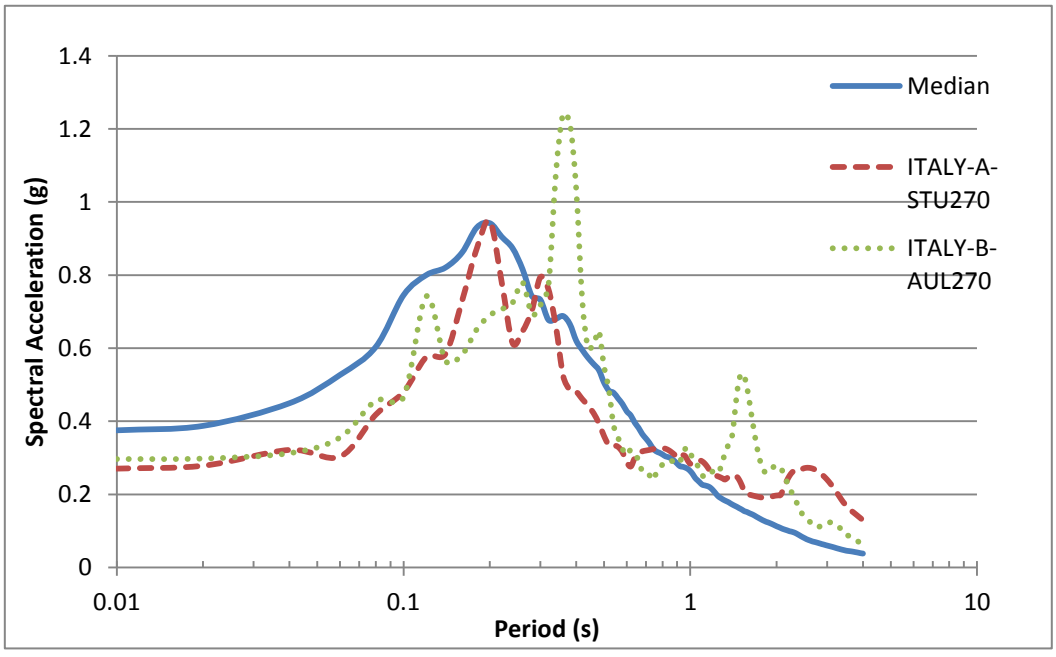

Figure 4.6 Response Spectra of two scaled motions with high S_a values in long-period range (T>1.0s)

Table 4.4 Decoupled Displacement of Motions Scaled and Matched to Target Response Spectrum for Site E (T_S=1.51s)

Earthquake Record	Scaled Motion (cm)	Matched Motion (cm)	Displacement Ratio
CHICHI06-TCU076-E	0.257	0.017	0.066
ITALY-A-AUL270	0.721	0.049	0.068
ITALY-A-BAG000	1.339	0.108	0.081
ITALY-A-STU270	**5.295**	**0.003**	**0.001**
ITALY-B-AUL270	**1.67**	**0.008**	**0.005**
KOZANI-KOZ--L	0.226	0.159	0.704
LOMAP-G01000	0.231	0.127	0.550
LOMAP-GIL067	0.265	0.344	1.298
MORGAN-GIL337	0.118	0.173	1.466
NORTHR-H12180	0.137	0.07	0.511
NORTHR-HOW330	0.125	0.048	0.384
NORTHR-LV1000	0.299	0.055	0.184
NORTHR-LV3090	1.315	0.34	0.259
NORTHR-WON185	0.37	0.05	0.135
VICT-CPE045	0.036	0.023	0.639
Median	0.37	0.06	0.15

As explained before, the small displacement for the long period site is caused by k_{max} being close to $k_y = 0.05g$. Increasing or decreasing the value of k_y will affect the relative displacement amplitude between the scaled motions and spectrally matched motions. To investigate the effect of k_y on the displacements, two other comparisons of sliding displacements with $k_y = 0.01g$ and $k_y = 0.1g$ are performed.

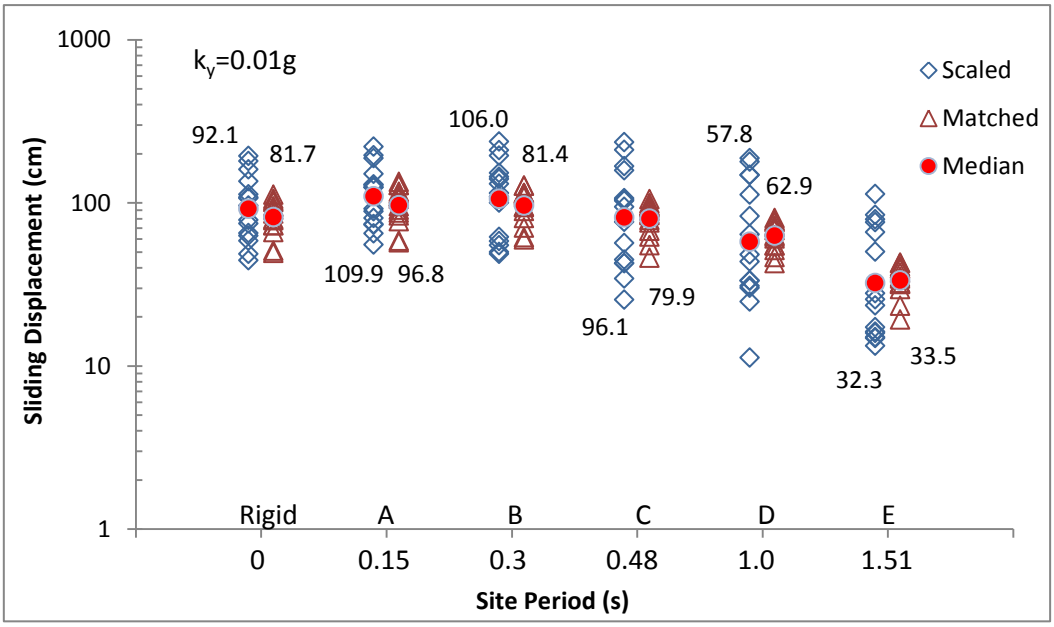

Figure 4.7 The displacement distribution of Motions Scaled and Matched to Target Response Spectrum (k_y=0.01g)

Table 4.5 Standard Deviation of Natural Logarithm of Displacements of Motions Scaled and Matched to Target Response Spectrum (k_y=0.01g)

	Rigid		Site A		Site B		Site C		Site D		Site E	
	S	M	S	M	S	M	S	M	S	M	S	M
σ_{lnD}	0.466	0.251	0.426	0.265	0.541	0.250	0.689	0.239	0.843	0.198	0.769	0.222

S: scaled motion **M**: matched motion

The computed displacements for $k_y = 0.01g$ are shown in Figure 4.7 for each site. The displacements are much larger than for $k_y = 0.05g$ due to the smaller k_y level. Additionally, the standard deviation of the natural logarithmic of the displacements (Table 4.5) shows the spectrally matched motions with standard deviation 40% to 70 % smaller than the scaled motions. Site E (Ts = 1.5 s) now has scatter that is similar to the other sites because k_{max} is no longer similar to k_y.

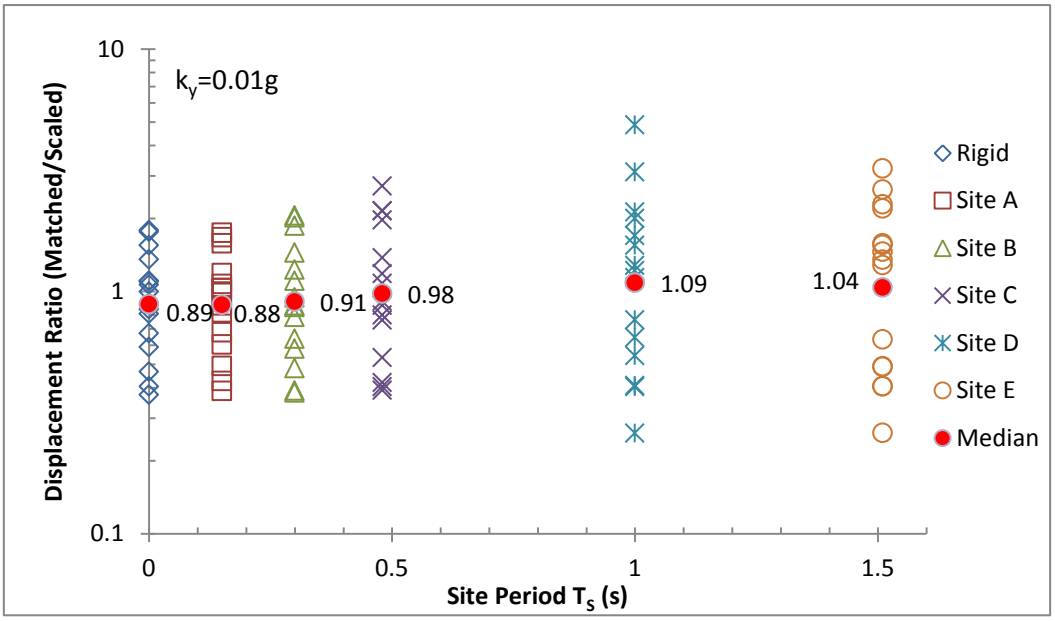

Figure 4.8 Displacement ratio of Motions Scaled and Matched to Target Response Spectrum for each site (k_y=0.01g)

The displacement ratios are shown in Figure 4.8. At the smaller k_y level, the average displacement ratios are within 0.89 to 1.09 for all site periods. Thus, the spectrally matched motions produce average displacements within about +/- 10% of the scaled motions. For $T_S \leq 1.0s$, the displacement ratios for $k_y = 0.01g$ are generally 10% to 20% larger than those from $k_y = 0.05g$ (Figure 4.3 and Figure 4.8). However, for $T_S = 1.5s$, the displacement ratios for $k_y = 0.01g$ are much larger than for $k_y = 0.05g$. The small displacement ratios for Ts = 1.5 s and k_y=0.05 g were a result of k_{max} being close to k_y, and now with k_y smaller the displacement ratios for this site are more in-line with the others.

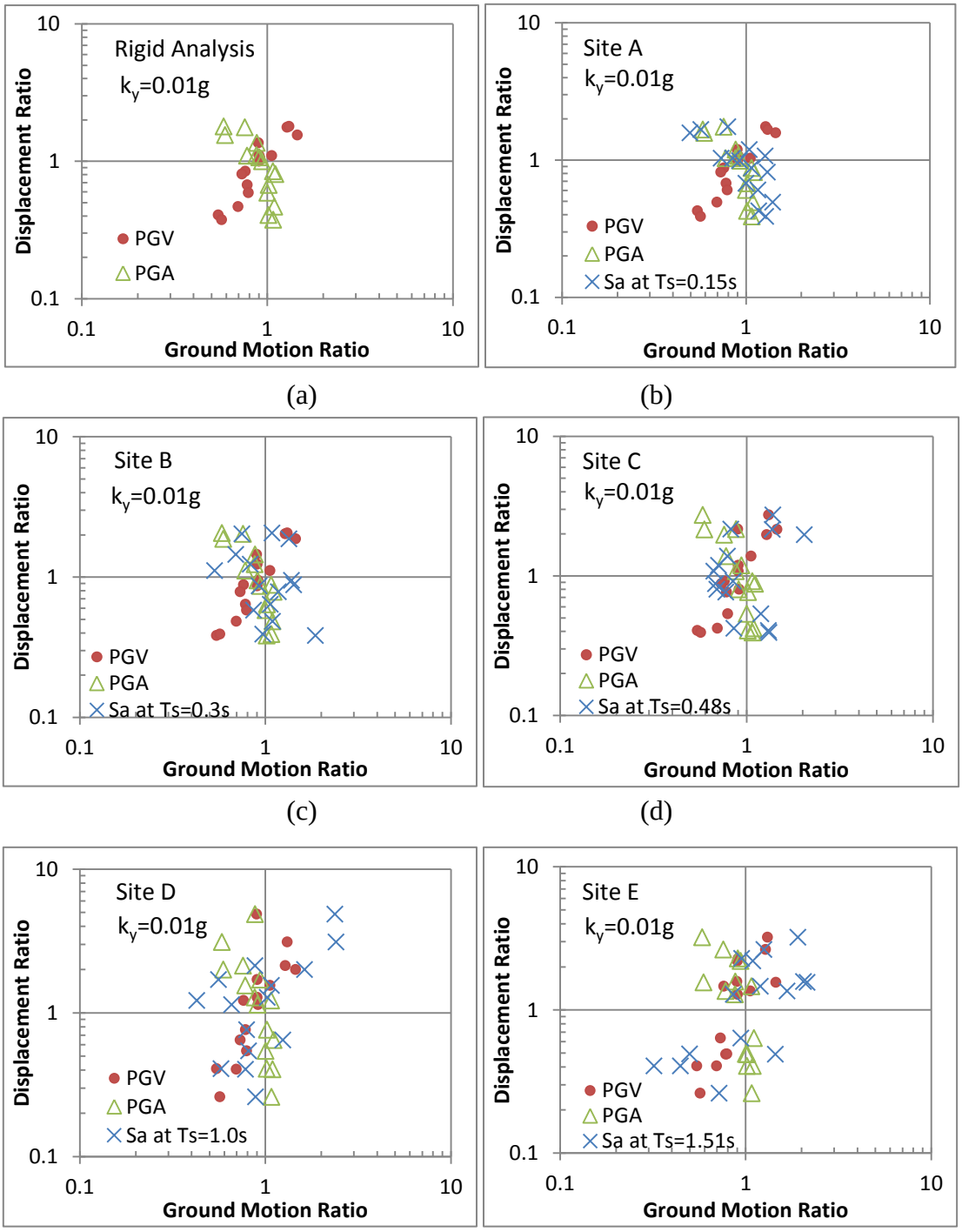

Figure 4.9 Ground Motion Ratios (matched/scaled) vs. Displacement Ratio (matched/scaled) for Motions Scaled and Matched to Target Response Spectrum for (a) Rigid, (b) Site A, (c) Site B, (d) Site C, (e) Site D, (f) Site E (k_y=0.01g)

To further investigate this explanation, the displacement ratios for $k_y = 0.01g$ are plotted versus ground motion ratios in Figure 4.9. Comparing Figure 4.9 ($k_y = 0.01g$) and Figure 4.5 ($k_y = 0.05g$), the displacement ratios for Sites A through C appear similar. For Sites D and E, the displacement ratios are concentrated in the range from 0.1 to 10 for $k_y = 0.01g$, but they fall between 0.0001 and 2 for $k_y = 0.05g$. The differences are caused by the fact that k_{max} is no longer close to the k_y level, and the computed sliding displacements of the spectrally matched motions do not have extremely small values as before.

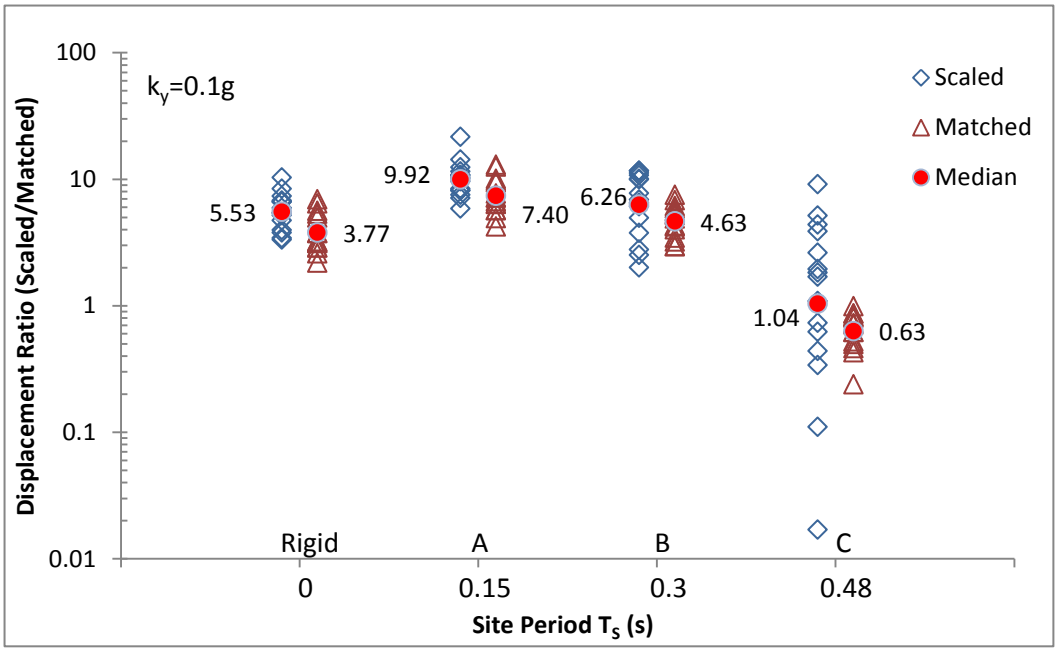

Figure 4.10 The Displacement Distribution of Motions Scaled and Matched to Target Response Spectrum for each site (k_y=0.1g)

Table 4.6 Standard Deviation of Natural Logarithm of Displacements Motions Scaled and Matched to Target Response Spectrum for each site (k_y=0.1g)

	Rigid		Site A		Site B		Site C	
	S	M	S	M	S	M	S	M
σ_{lnD}	0.330	0.349	0.316	0.329	0.597	0.299	1.630	0.370

S: scaled motion **M**: matched motion

To complete the investigation of k_y effects, the sliding displacements with $k_y = 0.1g$ were computed. The sliding displacements for $k_y = 0.1g$ are shown in Figure 4.10. Sites D and E are not shown because the displacements for most motions are zero because k_{max} is less than k_y. The displacements are much lower (only several centimeters) due to a higher k_y level ($k_y = 0.1g$). The larger k_y level causes smaller median displacement ratios in all period range as shown in Figure 4.11.

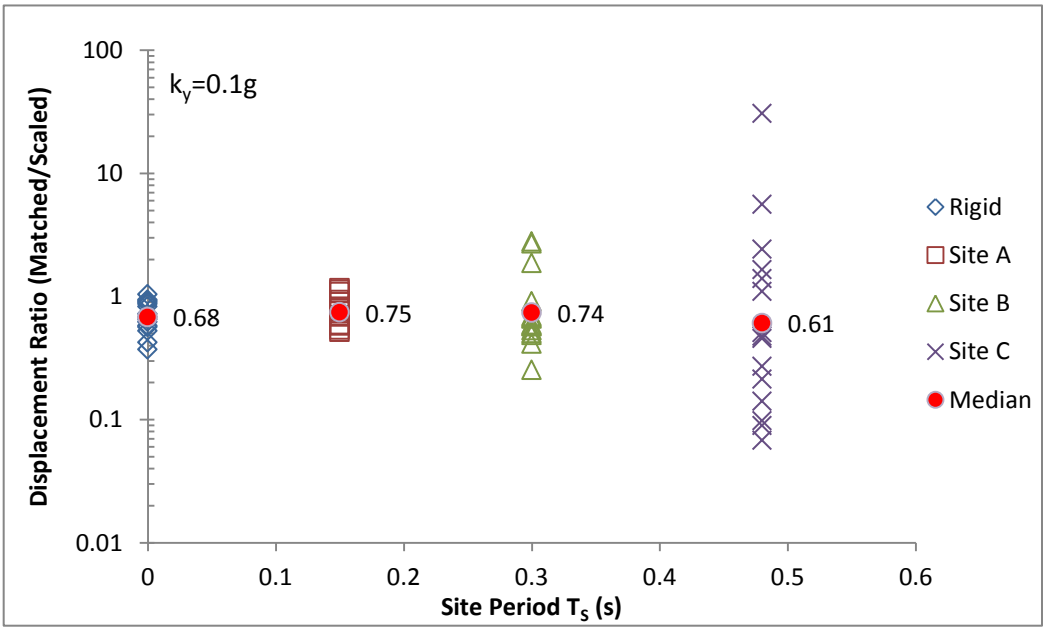

Figure 4.11 Displacement ratio of Motions Scaled and Matched to Target Response Spectrum each site (k_y=0.1g)

To further understand how the k_y value affects the differences between the displacement ratio, the Rathje and Antonakos (2010) model is again employed. The k_{max} and k-vel_{max} values from Table 4.3 were used in the displacement models for flexible sliding proposed by Rathje and Antonakos (2010). Displacements were computed for k_y =0.01, 0.05, 0.06, 0.07, 0.1 g. The k_{max} and k-vel_{max} values in Table 4.3 represent the best estimate in how the differences in the median input PGA, the median input PGV, and the median input T_m between the two suites of input motions affect the dynamic responses of the sliding masses. Using the displacement models allows for the differences in the median displacement ratios to be assessed. The computed displacement ratios are plotted versus k_y/k_{max} in Figure 4.12 for all the k_y values considered. Only the k_{max} values of the spectrally matched motions are used to compute k_y/k_{max}, because the difference between the k_{max} values of the spectrally matched and the scaled motions is quite small (about 10%) and consistent for all the sites (Table 4.3). There is a clear relationship between displacement ratio and k_y/k_{max}, with the ratio trending towards zero as k_y/k_{max} approaches 1.0. At large k_y/k_{max} the displacement level is controlled predominantly by the proximity of k_y to k_{max}, and with the matched motions inducing smaller values of k_{max} (Table 4.3) the displacement ratio gets very small. At smaller k_y/k_{max}, the displacement level is controlled by a combination of factors, such that the smaller responses for the spectrally matched motions (Table 4.3) leads to only a 15 to 30% reduction in displacement.

Thus, k_y/k_{max} plays a significant role in the displacement differences between the spectrally matched and scaled input motions.

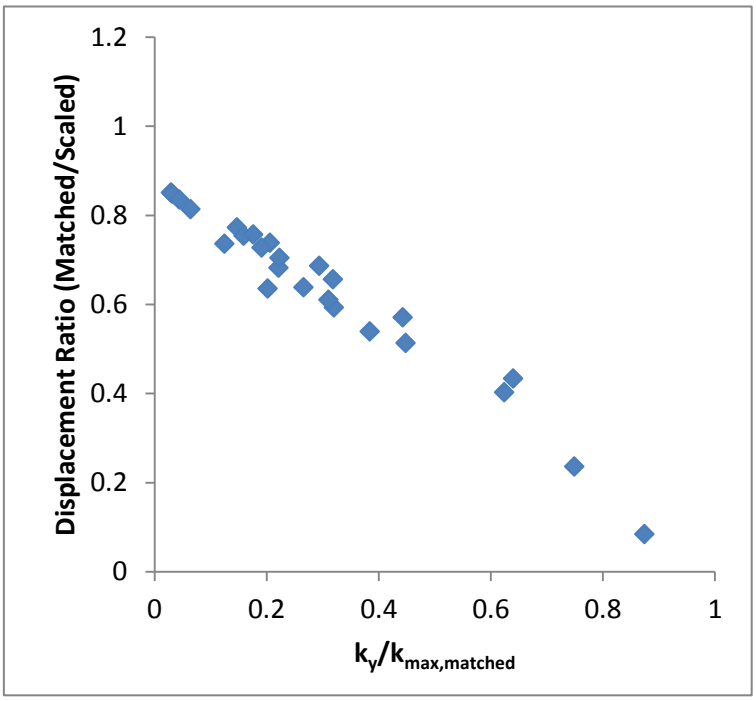

Figure 4.12 Displacement Ratio vs. k_y/k_{max} as Derived from Rathje and Antonakos (2010) Model Using Median Ground Motion Parameters of the Input Motion Suites and k_y = 0.01, 0.05, 0.06, 0.07, and 0.1 g.

4.3 SCALED AND MATCHED MOTIONS TO FIT TARGET RESPONSE SPECTRUM AND PGV

As shown in the previous section, the PGV has a significant influence on the displacement ratio. So it is necessary to perform a further comparison of sliding displacements for the case in which the spectrally matched motions are further modified to fit both the target response spectrum and the PGV of the suite of the scaled

motions. This modification was described in Section 3.3.3.

The median PGV values of the scaled and spectrally matched motions indicated the scaled motions had an average PGV that was 14% larger (i.e. a ratio of 1.14). A scale factor of 1.14 was applied to each of the spectrally matched motions, such that the median PGV of the spectrally matched motions was the same as the median PGV of the scaled motions. The scale factor also affects PGA such that the PGA of the matched motions now better compares to that of the scaled motions. The PGA ratio is now equal to 1.02, while the differences in T_m are unchanged because scaling does not affect T_m.

In Figure 4.13, the computed rigid and flexible sliding displacements of the scaled and spectrally matched motions are shown individually. Comparing the results in Figure 4.13 with those in Figure 4.1, the computed sliding displacements of the spectrally matched motions are now larger due to the increased intensity of these motions.

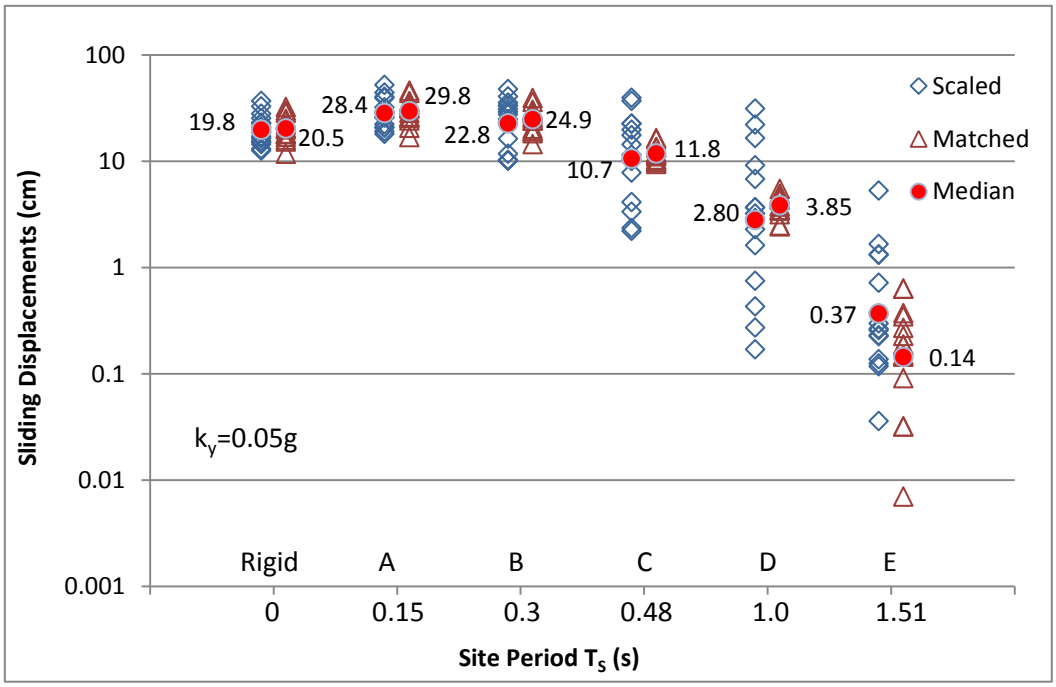

Figure 4.13 The Displacement Distribution of Motions Scaled and Matched to Target Response Spectrum and PGV for Each Site (k_y=0.05g)

Figure 4.14 shows the distribution of displacement ratio at each site. Compared with Figure 4.3 (where the spectrally matched motions were of lower intensity), the median displacement ratios in the short-period range ($T_S < 0.5s$) are now around 1.0 (ranging from 1.03 to 1.11) after correcting for the differences in median PGA and PGV of the scaled and spectrally matched motions. The displacement ratios in Figure 4.14 are generally 25% to 30% larger than those from Figure 4.3 for $T_S \leq 0.5$s. However, for $T_S = 1.0$s and 1.5s, the displacement ratios in Figure 4.14 are much larger than those in Figure 4.3. The displacement ratio for Ts = 1.0 s is now well above 1.0 and it is 70% larger than the value from Figure 4.3. The displacement ratio may be larger for

this site because the modification of the spectrally matched motions results in a larger S_a at T = 1.0 s (Figure 3.4). In particular, three motions (LOMAP-G01000, MORGAN-GIL337 and NORTHR-H12180) have very high displacement ratios. Considering most displacement ratios are in the range from 0.1 to 10 (Figure 4.14), these three motions with displacement ratios larger than 10, significantly increase the median displacement ratio. Figure 4.15 shows that the acceleration response spectra of these three scaled motions are much lower than the median response spectrum at periods greater than 0.5s, which leads to very small displacements for the scaled motions. Additionally, the PGV values for two of the scaled motions (MORGAN-GIL337 and NORHTR-H12180) are much smaller than for the spectrally matched motions (~ 15 cm/s vs. ~ 28 cm/s, Table 3.4), which contribute to the smaller displacements for the scaled motions.

For Ts = 1.5 s, the displacement ratio is still well below 1.0, but it is about 2.5 times larger than in Figure 4.3. The ratio is still less than 1.0 because k_{max} is still in the proximity of k_y.

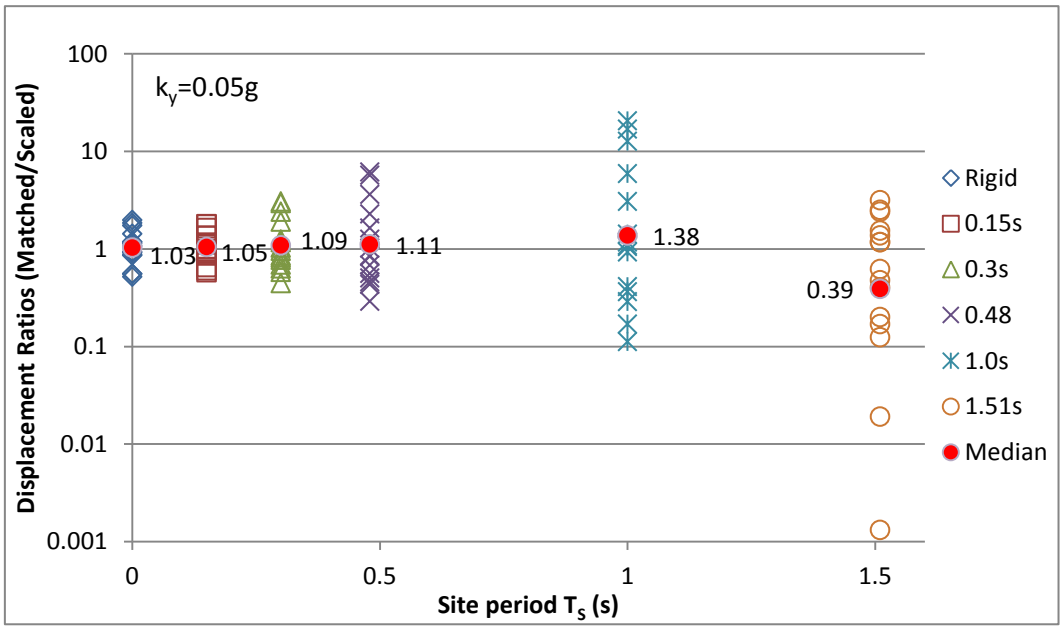

Figure 4.14 Displacement Ratios of Motions Scaled and Matched to Target Response Spectrum and PGV for Each Site (k_y=0.05g)

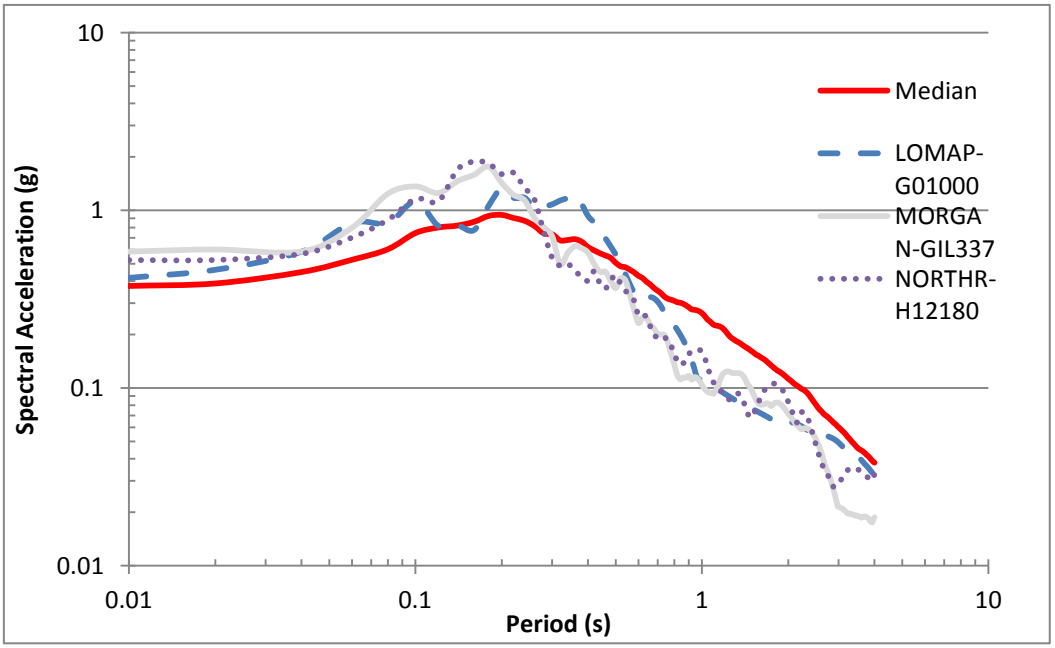

Figure 4.15 Response Spectra of Three Scaled Motions with Low S_a Values in Long-period Range (T>0.5s)

Table 4.7 Decoupled Displacement of Motions Scaled and Matched to Target Response Spectrum and PGV for Site D (T_S=1.0s)

Earthquake Record	Scaled Motion (cm)	Matched Motion (cm)	Displacement Ratio
CHICHI06-TCU076-E	2.297	2.436	1.061
ITALY-A-AUL270	6.802	2.485	0.365
ITALY-A-BAG000	16.59	4.791	0.289
ITALY-A-STU270	31.279	3.501	0.112
ITALY-B-AUL270	22.187	3.754	0.169
KOZANI-KOZ--L	1.617	4.971	3.074
LOMAP-G01000	**0.432**	**5.5**	**12.731**
LOMAP-GIL067	2.926	3.178	1.086
MORGAN-GIL337	**0.272**	**4.599**	**16.908**
NORTHR-H12180	**0.17**	**3.513**	**20.665**
NORTHR-HOW330	0.748	4.424	5.914
NORTHR-LV1000	3.686	3.421	0.928
NORTHR-LV3090	9.159	3.774	0.412
NORTHR-WON185	3.217	4.574	1.422
VICT-CPE045	3.696	4.357	1.179
Median	2.80	3.85	1.38

To again understand how the changes in the input ground motion parameters for the spectrally matched motions affect the dynamic response of the sliding masses, the Rathje and Antonakos (2010) model is employed. The predicted k_{max} and k-vel_{max} values are shown in Table 4.8 for the median ground motion parameters for the scaled motions and the modified spectrally matched motions. Increasing the intensity of the spectrally matched motions to match the PGV of the scaled motions results in the k_{max} and k-vel_{max} values being more similar between the two ground motion suites; however, the spectrally matched motions are still predicting smaller values, particularly

at longer periods. This smaller dynamic response is again directly caused by the smaller T_m values for the spectrally matched motions (Table 3.4). Nonetheless, the sliding displacement calculations in Figure 4.14 show that the matched motions are generally producing larger displacements for T_S less than or equal to 1.0 s. It is not clear why these displacements are now larger.

Table 4.8 Predicted Dynamic Response Parameters Using Rathje and Antonakos (2010) Model for Motions Scaled to Target Response Spectrum and PGV

Site Period (s)	k_{max} (g)			k-vel_{max} (cm)		
	Matched	Scaled	Ratio	Matched	Scaled	Ratio
0.15	0.342	0.350	1.02	29.42	29.4	1.00
0.3	0.243	0.258	0.98	27.80	28.6	1.00
0.48	0.172	0.188	0.94	24.58	25.8	0.97
1.0	0.085	0.096	0.92	17.67	19.2	0.95
1.51	0.052	0.060	0.88	13.65	15.1	0.92

The effect of k_y on the computed displacements and displacement ratios is investigated by performing analysis for k_y = 0.01 g and 0.1 g. Figure 4.16 shows the displacement ratio for each site, and these median values are larger than for k_y = 0.05 g. This increase in displacement ratio with a decrease in k_y was also observed for the motions scaled to the acceleration response spectrum (Figure 4.8) and is caused by the reduction in k_y/k_{max}. All of the median displacement ratios are greater than 1.0 for k_y = 0.01 g (i.e., the spectrally matched motions predict larger displacements than the scaled

motions). Comparing Figure 4.16 and Figure 4.14, the displacement ratios for rigid site and Site A through Site D appear similar. For Site E, the displacement ratios concentrated in the range from 0.1 to 10 for $k_y = 0.01g$, so the median displacement ratio goes up due to k_{max} being away from k_y level.

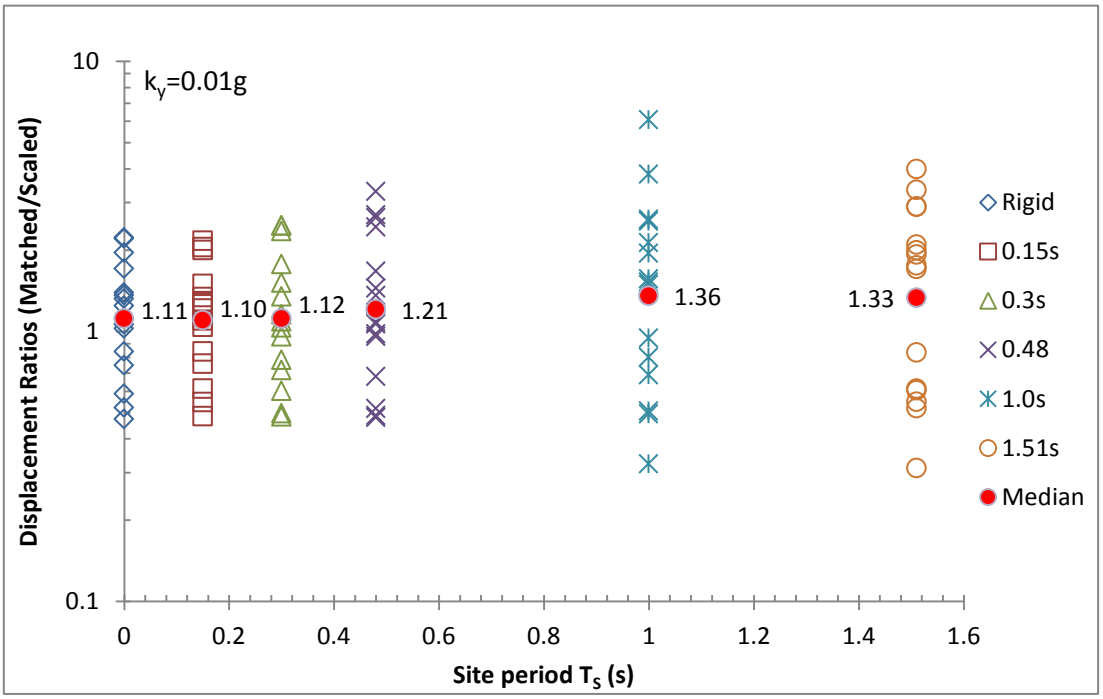

Figure 4.16 Displacement ratio of Motions Scaled and Matched to Target Response Spectrum and PGV for each site (k_y=0.01g)

The displacement ratios for $k_y = 0.1g$ are shown in Figure 4.17. Displacement ratios for Sites D and E are not shown because for these sites k_{max} is less than k_y. At this higher k_y level, the median displacement ratios are all greater than 1.0, but they are all less than 1.1.

Comparing the results from the three k_y values, the median displacement ratios seem very consistent in the short period range (i.e., most displacement ratios between 1.0 and 1.1 for $T_S \leq 0.5s$). The sliding displacements of the spectrally matched motions are generally 5% to 10% higher than the scaled motions. Considering that the median PGA and PGV values of these two suites of motions are similar (Table 3.4) and also the predicted k_{max} and k-vel_{max} are similar (Table 4.8), it is possible that the differences in S_a (Figure 3.4) should cause this trend.

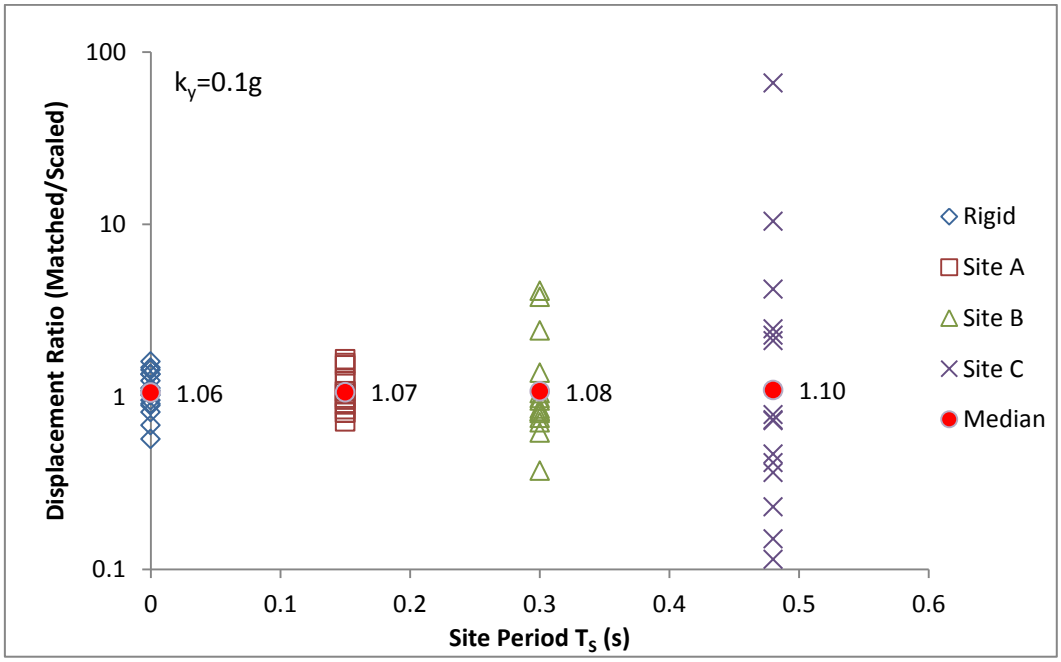

Figure 4.17 Displacement Ratio of Motions Scaled and Matched to Target Response Spectrum and PGV for each site (k_y=0.1g)

4.4 SCALE MOTIONS AT A CERTAIN SITE PERIOD TO FIT TARGET RESPONSE SPECTRUM

Some engineers may focus on scaling their motions to fit the target response spectrum exactly at the period of the site being analyzed. This scaling method attempts to ensure that the intensity of the motion in the period range close to T_s is captured well. Site D, which has a natural period $T_S = 1.0s$, is investigated to compare motions scaled to the target response spectrum and motions scaled to S_a at the site period. Only the suite of linearly scaled motions was considered.

The target S_a at T = 1.0 s is equal to 0.252 g (Figure 3.5). To make each motion fit the target response spectrum at $T = 1.0s$, each response spectrum is scaled by a factor that results in S_a = 0.252 g at T = 1.0 s. This scaling process has been described in Section 3.3.4. As seen in Figure 3.5, the acceleration response spectra of all of the motions go through the same value at $T_S = 1.0s$, but they are distributed more widely at all other periods (Figure 3.7). It is interesting to note that the suite of these newly scaled motions still has a median response spectrum very similar to the target.

The displacements calculated for Site D subjected to the motions scaled to fit the target response spectrum and the motions scaled to fit S_a at T=1.0s are shown in Figure 4.18 for k_y=0.05 g. It is interesting that the suite of these newly scaled motions has not only a similar median sliding displacement as before (~2.8 cm), but also has a

similar standard deviation of sliding displacement after minimizing their acceleration response spectra at the site period. The similar median sliding displacement is due to similar median PGA, PGV (Table 3.5) and S_a (Figure 3.6) values for the two suites. The similar standard deviation of the sliding displacements is not controlled by the spectral accelerations at $T_s = 1.0s$, but rather the range of all of the ground motion parameters including PGA and PGV. Additionally, due to soil nonlinearity earthquake shaking causes the site period to lengthen such that Site D would no longer have a site period equal to 1.0 s Thus, the standard deviation of the sliding displacements should also be affected by S_a at longer periods (e.g. $T_s = 1.51s$) and by PGV (as investigated in Figure 4.5 and Figure 4.9). The standard deviations of the displacement and ground motion parameters are listed in Table 4.9.

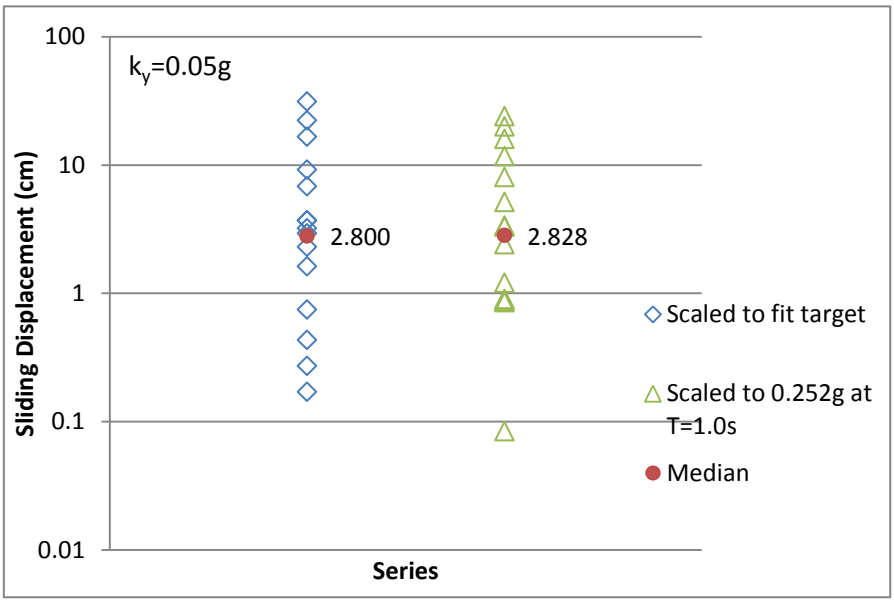

Figure 4.18 The Displacement Distribution of Motions Scaled to 0.252g at T=1.0s and Scaled to Target Response Spectrum (k_y=0.05g)

Table 4.9 Standard Deviation of Natural Logarithm of Displacements Motions Scaled to Target Response Spectrum and Scaled to 0.252g at T=1.0s for each site (k_y=0.05g)

	Sliding Displacement		S_a at 1.0s		S_a at 1.51s		PGV		PGA	
	S	S1	S	S1	S	S1	S	S1	S	S1
σ_{lnD}	1.570	1.547	0.491	0.000	0.571	0.508	0.260	0.452	0.240	0.663

S: Scaled to Target Response Spectrum **S1**: Scaled to 0.252g at $T = 1.0s$

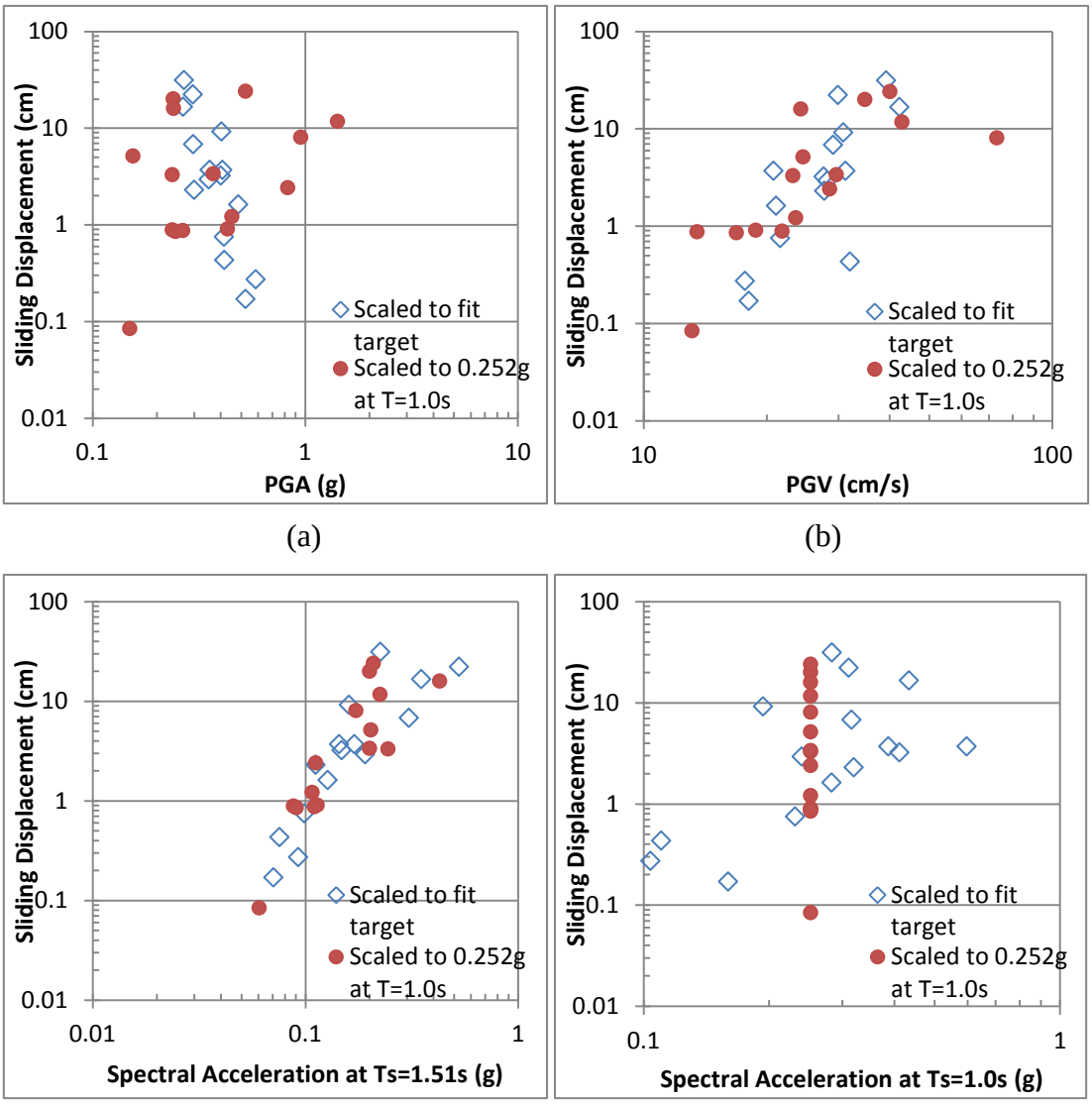

Figure 4.19 Ground Motions vs. Sliding Displacements of Motions Scaled to 0.252g at T=1.0s and Scaled to Target Response Spectrum (a) PGA (b) PGV (c) Spectral Acceleration at T_S=1.51s and (d) Spectral Acceleration at T_S=1.0s (k_y=0.05g)

Figure 4.19 plots the displacement ratios versus ground motion ratios of PGA, PGV, S_a at T = 1.0s, and Ts = 1.51 s in an effort to investigate which ground motions are controlling the displacement variability. Figure 4.19 shows that PGV and the

spectral acceleration at $T_S = 1.51s$ correlates with the sliding displacement better than PGA and spectral acceleration at $T_S = 1.0s$. These data indicate that S_a at longer periods and PGV are influencing the variability in displacement. Table 4.9 shows that the standard deviation for S_a at 1.5 s is similar for both of the suites, indicating that this ground motion parameter may have the largest influence on the variability in displacement for this case.

4.5 EMPIRICAL PREDICTION

In Section 4.2 and 4.3, empirical predictive models from Antonakos and Rathje (2010) were used for explaining the k_y effects. In this Section, a further investigation into the empirical prediction of displacement is performed.

Using the median parameters (from Table 3.3) of the scaled and spectrally matched motions as input into the Rathje and Antonakos (2010) models, the predicted values of k_{max}, k-vel_{max} and sliding displacement are shown in Figure 4.20.

Table 4.10 Input Median Parameters for Rathje and Antonakos (2010) Models

Median Parameters	Scaled Motions	Matched Motions
PGA (g)	0.375	0.337
PGV (cm/s)	27.0	23.6
T_m (s)	0.43	0.38

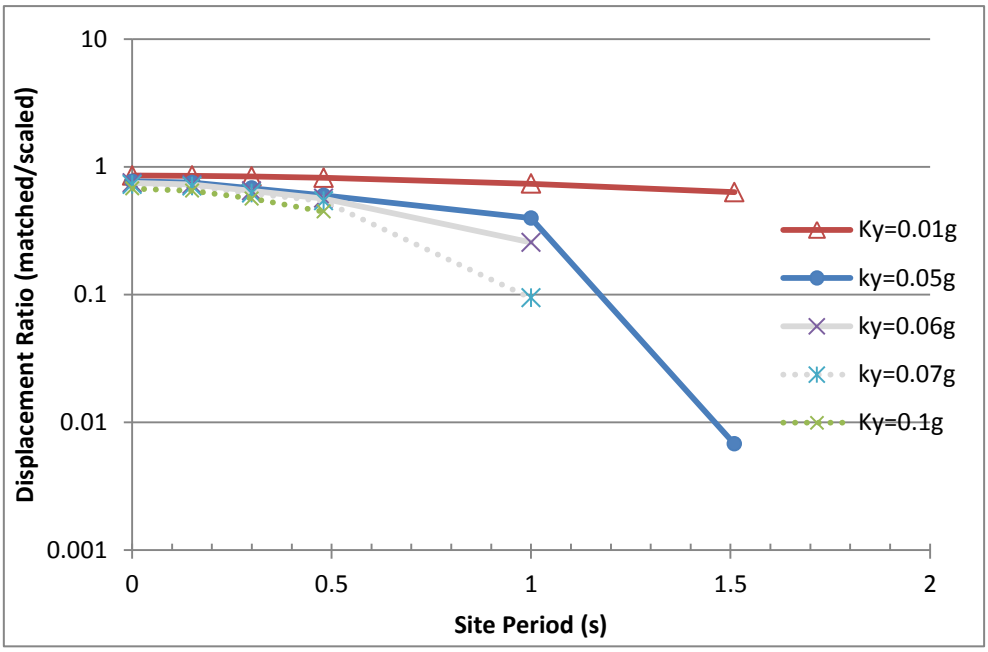

Figure 4.20 k_y Effects on the Displacement Ratio Predicted by Rathje and Antonakos (2010) Models

Compared with the displacement ratios computed in this study and shown in Figure 4.3, Figure 4.8 and Figure 4.11, the predicted displacement ratios (Figure 4.20) are smaller than the computed values given by rigorous analyses. However, the general trends regarding how k_y affects the displacement ratio are very similar between the empirical prediction and computed values.

Figure 4.20 shows that the displacement ratio for each site increases with decreasing k_y. And in the long-period range, the k_y effects are more significant than in the short-period range due to k_{max} being close to k_y in the long period range. In this case, changing k_{max} leads to more influence on the displacement. The results of the empirical predictive models verify the observations from before.

Figure 4.21 shows the individual predicted displacement ratio from Rathje and Antonakos (2010) for each motion fit to the acceleration response spectrum. The input parameters PGA, PGV and T_m are from Table 3.3. Sites D and E are not shown in this figure, because several motions induced zero displacements. Compared with the computed displacement ratio for each individual motion, the difference in displacement ratios is within 5% at $T_S \leq 0.3s$ and about 10% at $T_S = 0.5s$.

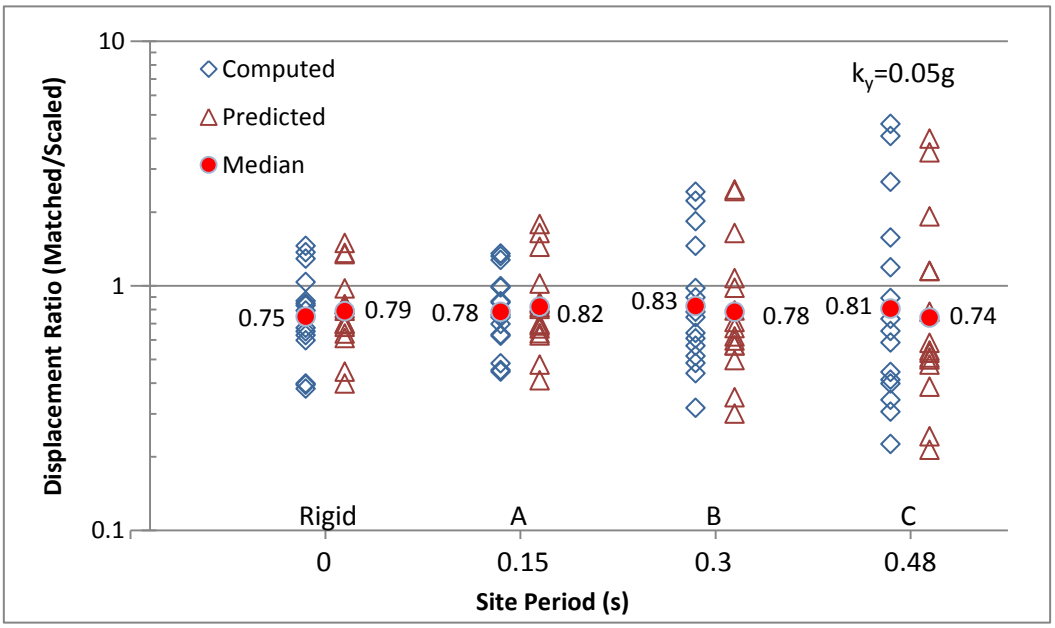

Figure 4.21 Predicted Displacement Ratios vs. Computed Displacement Ratios of Motions Scaled and Matched to Target Response Spectrum for Each Site (k_y=0.05g)

One additional consideration should be noted when comparing the results of Rathje and Antonakos (2010) and this study. Rathje and Antonakos (2010) used

layered, equivalent-linear soil profiles for their computation of k-time histories, and the nonlinear property curves defined based on the model of Stokoe and Darendeli (2001) with PI=0 and a depth dependent confining pressure. The program SLAMMER uses the simplified modal analysis with only one layer and the nonlinear property curves are defined by Stokoe and Darendeli (2001) with PI equal to 30 (Lee, 2004). A higher PI leads to less nonlinear behavior in soil, so the Antonakos and Rathje (2010) models predicted somewhat more nonlinearity in the dynamic response (i.e., smaller k_{max} and k-vel_{max}) than the decoupled analysis in SLAMMER. This difference may explain the smaller displacement ratios computed using the Rathje and Antonakos (2010) model.

Chapter 5 Conclusions

5.1 SUMMARY

This thesis presented a series of comparisons to investigate the influence of ground motion scaling methods on the seismically-induced sliding displacements of slopes. Two main approaches to ground motion selection were considered: linear scaling of recorded ground motions and modification of recorded ground motions through spectral matching. A suite of 15 motions was initially selected and scaled to fit a target acceleration response spectrum, and these motions were then spectrally matched such that each motion had a response spectrum similar to the target spectrum. Matching a target acceleration response spectrum is commonly the only criterion used when assessing a suite of ground motions, although additional ground motion parameters (e.g., peak ground velocity) can be used to characterize ground motions. The scaled and spectrally matched suites of motions used in this study displayed very similar response spectra, but their peak ground velocities were different. Therefore, an additional comparison was made in which the suites were scaled to better match the PGV. Finally, a subset of analyses was performed using the linearly scaled suite of motions and another suite consisting of all of the motions scaled directly to the spectral acceleration at a specific period.

Sliding displacements were computed by rigid sliding-block analysis and

decoupled sliding-block analysis. The rigid analyses represent sliding for shallow failure surfaces where the dynamic response of the sliding mass can be ignored, while the decoupled analyses represent deeper, one-dimensional sliding masses in which the dynamic response is computed and used in the sliding displacement calculation. The decoupled sliding masses were modeled with natural periods of 0.15, 0.3. 0.5, 1.0, and 1.5 s. Yield accelerations of 0.01 g, 0.05 g, and 0.1 g were considered. All analyses were performed with the program SLAMMER (developed by Jibson et al.), which incorporates a simplified, equivalent-linear, modal model for the dynamic response of the sliding mass. Comparisons were made by computing the displacement ratio, defined as the displacement computed for a spectrally matched motion divided by the displacement computed for the corresponding scaled motion. The median displacement ratio was computed for each suite of motions. Empirical predictive models are included for explaining the k_y effect and comparing with those rigorous sliding displacement analyses were also employed to investigate the results obtained from the suites of acceleration-time histories.

5.2 CONCLUSIONS

The displacements computed from the spectrally matched motions were generally 10 to 30% smaller, on average, than the displacements computed from the linearly scaled motions when both suites of input motions were developed to match the

same acceleration response spectrum. For sites with longer natural periods (~1.5 s), the spectrally matched motions may predict displacements as much as 70% smaller than scaled motions. These differences are more pronounced as the ratio of k_y/k_{max} approaches 1.0 (either due to large k_y or small k_{max}), and the differences are driven predominantly by differences in peak ground velocity between the suites of scaled and spectrally matched motions. Additionally, the displacements predicted by the spectrally matched motions display significantly less variability than the displacements from the scaled motions due to less variability in the input motion suite.

When the spectrally matched motions were increased in intensity to match better the median PGV of the scaled motions, these motions predicted displacements from 5 to 15% larger, on average, than the displacements from the scaled motions for site periods less than or equal to 0.5 s. At longer periods, the differences were as large as 40%. The differences were most substantial as k_y was reduced. For these analyses, the PGV of the two suites of motions matched better and the median displacements were more similar; however, the spectrally matched motions now systematically predicted larger displacements than the scaled motions.

The comparisons between scaled and spectrally matched motions indicate that these types of motions can produce significantly different estimates of sliding displacement. For the suites of motions considered in this study, if the PGV of the spectrally matched motions are smaller than those of the scaled motions, the spectrally

matched motions will predict smaller displacements than the scaled motions. However, if the spectrally matched motions are scaled to better match the PGV of the scaled motions, they tend to predict displacements that are larger than the displacements of the scaled motions. For most cases, the median displacements from the suite of spectrally matched motions were within +/- 30% of the median displacement of the suite of scaled motions.

Because ground motion parameters beyond the response spectrum affect the computed sliding displacement, these ground motion parameters should be considered when selecting and scaling input motions. PGA and PGV have large influences on the rigid sliding displacements, and the corresponding parameters k_{max} and k-vel_{max}, affect the displacement of flexible sliding masses. k_{max} and k-vel_{max} represent the dynamic response of the sliding mass and are affected by the PGA, PGV, and mean period (T_m) of the input ground motions. Thus, all three of these ground motion parameters should be considered in selecting and scaling motions for use in sliding displacement analyses.

Bibliography

Abrahamson, N. A. (1992). "Non-stationary spectral matching," Seismological Research Letters, Vol. 63(1), pp. 30.

Boore, D. M. and Atkinson, G. M. (2008). "Ground-motion prediction equation for average horizontal component of PGA, PGV, and 50.01s and 10.00s," Earthquake Spectra, Vol. 24(1), pp. 99-138.

Bray, J. D. and Rathje, E. M. (1998). "Earthquake-induced displacements of solid-waste landfills," Journal of Geotechnical Engineering 124, pp. 242-253.

Close, U. and McCormick, E. (1922). "Where the mountains walked," National Geographic, Vol. 41, No. 5, pp. 445-464.

Darendeli, M. B. and Stokoe II, K. H. (2001). "Development of a new family of normalized modulus reduction and material damping curves," Geotechnical Engineering Report. GD01-1, University of Texas, Austin, Texas.

Hancock, J., Watson-Lamprey, J., Abrahamson, N., Bommer, J., Markatis, A., McCoy, E. and Mendis, R. (2006). "An improved method of matching response spectra of recorded earthquake ground motion using wavelet," Journal of Earthquake Engineering, Vol. 10, pp. 67-89.

Jibson, R. W. (1993). "Predicting earthquake-induced landslide displacements using Newmark's sliding block analysis," Transportation Research Record 1411. Transportation Research Board, Washington, D.C., pp. 9-17.

Jibson, R. W. (2010). "Methods for assessing the stability of slopes during earthquakes – A retrospective," Engineering Geology, accepted for publication.

Keefer, D. K. (1984). "Landslides caused by earthquakes," Geologic Society of America Bulletin. Vol. 95, No. 2, pp. 406-421.

Kobatashi, Y. (1981). "Causes of fatalities in recent earthquakes in Japan," Journal of Disaster Science, Vol. 3, pp. 725-730

Kottke, A. and Rathje, E. M. (2008). "A semi-automated procedure for selecting and scaling recorded earthquake motions for dynamic analysis," Earthquake Spectra, Vol. 24, No. 4, pp. 911-932.

Kottke, A. and Rathje, E. M. (2010). "Comparison of random vibration theory and time series seismic site response analysis," Final Report submitted to the Nuclear Regulatory Commission.

Kramer, S. L. (1996). Geotechnical Engineering Earthquake, Upper Side River, N.J. 07468: Prentice-Hall Inc.

Lee, Y. W. (2004). "Equivalent-linear dynamic sliding response analysis of geotechnical earth structures," M.S. Thesis, Department of Civil, Architectural and Environmental Engineering, University of Texas, Austin, TX. 70 pp.

Lin, J. S. and Whitman, R. V. (1983). "Earthquake induced displacements of sliding blocks," Journal of Geotechnical Engineering 112, pp44-59.

Makdisi, F. I. and Seed, H. B. (1978). "Simplified procedure for estimating dam and embankment earthquake-induced deformation," Journal of the Geotechnical Engineering Division 104, pp. 849-867.

Newmark, N. (1965). "Effects of earthquake on dams and embankments," Geotechnique, Vol. 15, No.2, pp. 139-160.

Rathje, E. M. and Antonakos, G. (2010). "Recent advances in predicting earthquake-induced sliding displacements of slopes," Fifth International Conference on Recent Advances in Geotechnical Earthquake Engineering and Soil Dynamics. San Diego, California.

Rathje, E. M. and Bray, J. D. (1999). "An examination of simplified earthquake-induced displacement procedures for earth structures," Canadian Geotechnical Journal, Vol. 36(1), pp. 72-87.

Rathje, E. M. and Saygili, G. (2009). "Probabilistic assessment of earthquake-induced sliding displacements of natural slopes," Bulletin of the New Zealand Society for Earthquake Engineering, Vol. 42(1), pp. 18-27.

Saygili, G. and Rathje, E. M. (2008). "Empirical predictive models for earthquake-induced sliding displacements of slopes," Journal of Geotechnical and Geoenvironmental Engineering, ASCE, Vol. 134(6), pp. 790-803.

Seed, H. B, and Martin, G. R. (1966). "The seismic coefficient in earth dam design," Journal of the Soil Mechanics and Foundation Division, ASCE, Vol. 92. No. SM3, pp. 25-58.

Terzaghi, K. (1950). Mechanisms of landslides, Engineering Geology (Berkey) Volume, Geological Society of America.

Wilson, R. C. and Keefer, D. K. (1985). "Predicting areal limits of earthquake-induced landsliding," in Evaluating Earthquake Hazards in Los Angeles Region, Zinoy, J.L., ed., U.S. Geological Survey, Reston, Virginia, Professional Paper 1360, 317-345.

Youd, T. L. (1978). “Major cause if earthquake damage is ground failure,” Civil Engineering, ASCE, Vol. 48 NO. 4, pp. 47-51

Vita

Yubing Wang was born in Tangshan, China in 1987. After completing his study at Tangshan No. 1 High School, he was admitted by Tongji University, Shanghai, China, in 2005. His major was Civil Engineering. He earned the degree of Bachelor of Engineering from Tongji University in July 2009. In August 2009, he entered the Graduate School at The University of Texas at Austin.

Email: wangyubing1987@hotmail.com

This thesis was typed by the author.